T.R.N.C

NEAR EAST UNIVERSITY

GRADUATE SCHOOL OF HEALTH SCIENCES

INHIBITORY EFFECT OF HYPERICIN ON GLUTATHIONE REDUCTASE PURIFIED FROM BAKER'S YEAST

Redwan Kawa ABDULLAH

MEDICAL BIOCHEMISTRY PROGRAM

MASTER OF SCIENCE THESIS

NICOSIA

2017

T.R.N.C.
NEAR EAST UNIVERSITY
GRADUATE SCHOOL OF HEALTH SCIENCES

INHIBITORY EFFECT OF HYPERICIN ON GLUTATHIONE REDUCTASE PURIFIED FROM BAKER'S YEAST

Redwan Kawa ABDULLAH

MEDICAL BIOCHEMISTRY PROGRAM
MASTER OF SCIENCE THESIS

SUPERVISOR
Associate Professor Özlem DALMIZRAK

NICOSIA
2017

The Directorate of Graduate School of Health Sciences,

This study has been accepted by the thesis committee in Medical Biochemistry program as a Master of Science Thesis.

Thesis committee:

Chair: Professor Nazmi ÖZER
Near East University

Member: Professor Nevbahar TURGAN
Ege University

Supervisor: Associated Professor Özlem DALMIZRAK
Near East University

Approval:

According to the relevant article of the Near East University Postgraduate Study – Education and Examination Regulation, this thesis has been approved by the above mentioned members of the thesis committee and the decision of the board of Director of the Institute.

Professor İhsan CALIŞ
Director of the Graduate School of Health Sciences

ACKNOWLEDGEMENTS

First, I would like to express earnest appreciation to my supervisor Associate Professor Özlem Dalmızrak for her commitment, consolation, patience and support**.**

I am grateful to Professor Nazmi Özer for his instruction and support during my postgraduate study.

I am grateful to Professor Hamdi Öğüş for his valuable contribution.

I am grateful to my classmate Evelyn Asuquo who was stand by my side during our thesis.

Finally, my deepest expression to my father Kawa Abdullah and my mother Pakhshan Abdullah for their encouragement, support and patience during my education through all these years.

ABSTRACT

Abdullah R.K. Inhibitory Effect of Hypericin on Glutathione Reductase Purified from Baker's Yeast. Near East University, Graduate School of Health Sciences, M.Sc. Thesis in Medical Biochemistry Program, Nicosia, 2017.

Glutathione is the most common non-protein thiol peptide in almost all living organisms and has a role in antioxidant defense mechanisms and xenobiotic detoxification. Glutathione reductase (GR) is one of the enzymes that functions in regeneration of reduced glutathione (GSH) from oxidized glutathione (GSSG). Hypericin is a naturally occurring substance found in St. John's Wort (*Hypericum perforatum L.*). It has antidepressant, antiviral actions and is used in photodynamic therapy of several oncological diseases. In this study, the interaction of hypericin with GR (E C 1.6.4.2) purified from baker's yeast (*S. cerevisiae*) was investigated.

Activity measurements were carried out at 340 nm by using different [hypericin] at either fixed 1 mM [GSSG]-variable [NADPH] or fixed 0.1 mM [NADPH]-variable [GSSG]. On native and SDS-PAGE gels, GR gave a single protein and activity bands. Molecular weight of a single subunit was calculated as 49 kDa. The pH optimum was found to be 7.65 by zero buffer extrapolation method. The temperature optimum, activation energy and Q_{10} were calculated as 57^{o}C, 3,544 calories and 1.26, respectively. Hypericin was found to be as an effective inhibitor of GR with an IC_{50} value of 15 μM. When the variable substrate is GSSG, inhibition type was competitive, K_m and K_i were found as 190 ± 40 μM and 2.92 ± 0.73 μM, respectively. On the other hand, when the variable substrate was NADPH, inhibition type was linear-mixed type competitive and the K_s, K_i and α values were 15.8 ± 1.6 μM, 2.63 ± 0.50 μM and 3.48 ± 1.31, respectively. Competitive inhibition with GSSG clearly shows that hypericin binds to the GSSG binding site. On the other hand, linear-mixed type competitive inhibition with NADPH indicates that although hypericin binds to the GSSG site it is a huge molecule and it also affects the binding of NADPH because GSSG and NADPH sites are close to each other.

Keywords: Glutathione reductase, hypericin, inhibition kinetics, K_i

ÖZET

Abdullah R.K. Hiperisinin Ekmek Mayasından Saflaştırılan Glutatyon Redüktaz Enzimine İnhibe Edici Etkisi. Yakın Doğu Üniversitesi, Sağlık Bilimleri Enstitüsü, Tıbbi Biyokimya Programı, Yüksek Lisans Tezi, Lefkoşa, 2017.

Glutatyon bütün organizmalarda yaygın olarak bulunan protein olmayan tiyol peptididir ve antioksidan savunma mekanizmaları ve ksenobiyotik detoksifikasyonunda rolü bulunmaktadır. Glutatyon redüktaz (GR) okside glutatyonun (GSSG) redükte glutatyona (GSH) rejenerasyonunda görev yapmaktadır. Hiperisin St. John's Wort (*Hypericum perforatum L.*)'de bulunan doğal bir bileşiktir. Antidepresan, antiviral etkileri bulunmaktadır ve birçok onkolojik hastalığın fotodinamik tedavisinde kullanılmaktadır. Çalışmamızda hiperisin ile ekmek mayasından (*S. cerevisiae*) saflaştırılmış GR (E.C. 1.6.4.2) arasındaki etkileşim araştırılmıştır. Aktivite ölçümleri 340 nm'de farklı hiperisin derişimlerinde, sabit 1 mM [GSSG]-değişken [NADPH] ya da sabit 0.1 mM [NADPH]-değişken [GSSG] kullanılarak gerçekleştirilmiştir. Natif ve SDS-PAGE jellerinde GR tek bir protein ve aktivite bandı vermiştir. Altbirim molekül ağırlığı 49 kDa olarak hesaplanmıştır. pH optimumu sıfır tampon ekstrapolasyonu yapılarak 7.65 olarak bulunmuştur. Optimum sıcaklık, aktivasyon enerjisi ve Q_{10} sırasıyla 57^{o}C, 3,544 kalori ve 1.26 olarak hesaplanmıştır. Hiperisinin GR enzimini inhibe ettiği gözlenmiş ve IC_{50} değeri 15 μM olarak bulunmuştur. Değişken substrat GSSG olduğunda, hiperisin GR'yi kompetitif olarak inhibe etmektedir. K_m ve K_i değerleri sırasıyla 190 ± 40 μM ve 2.92 ± 0.73 μM olarak bulunmuştur. Diğer taraftan, NADPH değişken substrat olarak kullanıldığında inhibisyonun türü lineer karışık tip kompetitif olarak belirlenmiştir. K_s, K_i ve α değerleri 15.8 ± 1.6 μM, 2.63 ± 0.50 μM ve 3.48 ± 1.31 olarak hesaplanmıştır. Değişken GSSG ile gözlenen kompetitif inhibisyon hiperisinin enzimin GSSG bağlanma bölgesine bağlandığını; lineer karışık tip kompetitif inhibisyon ise büyük bir molekül olan hiperisinin NADPH'nin de bağlanmasını etkilediğini göstermektedir.

Anahtar Kelimeler: Glutatyon redüktaz, hiperisin, inhibisyon kinetiği, K_i

TABLE OF CONTENTS

ABBREVIATIONS

2-AAPA	: 2-acetylamino-3-[4-(2-acetylamino-2 carboxyethylsulfanyl thiocarbonylamino) phenylthiocarbamoylsulfanyl] propionic acid
AIDS	: Acquired Immune Deficiency Syndrome
APS	: Ammonium persulfate
BCNU	:1,3-bis (2-chloroethyl)-1-nitrosourea
BCRP	: Breast cancer resistance protein
BSA	: Bovine serum albumin
CAT	: Catalase
CBB	: Coomassie Brilliant Blue
CDNB	: 1-chloro-2,4-dinitrobenzene
CuZnSOD	: Copper/zinc superoxide dismutase
dH_2O	: Distilled water
DMSO	: Dimethyl sulfoxide
DNA	: Deoxyribonucleic acid
E. coli	: *Escherichia coli*
E_a	: Energy of activation
FAD	: Flavin adenine dinucleotide
G6P	: Glucose-6-phosphate
G6PD	: Glucose-6-phosphate dehydrogenase
GABA	: Gamma-aminobutyric acid
γ-GCG	: Gamma-glutamyl-cysteinyl-glycine
GCL	: Glutamate-cysteine ligase
GCLC	: Glutamate-cysteine ligase catalytic subunit
GCLM	: Glutamate-cysteine ligase modifier subunit
Glr1	: Yeast glutathione reductase
GPx	: Glutathione peroxidase
GR	: Glutathione reductase
GSH	: Reduced glutathione
GSSG	: Oxidized glutathione

GST	: Glutathione S-transferase
GST-α	: Glutathione S-transferase alpha
GST-π	: Glutathione S-transferase pi
H. sapiens	: *Homo sapiens*
H_2O_2	: Hydrogen peroxide
HNO	: Nitroxyl
$OH^{\cdot}$	: Hydroxyl radical
HOCl	: Hypoclorous acid
HPLC	: High-pressure liquid chromatography
IC_{50}	: Half maximum inhibitory concentration
*K*i	: Inhibitory constant
K_m	: Michaelis constant
K_s	: Dissociation constant
MAO	: Monoamine oxidase
MnSOD	: Manganese-superoxide dismutase
Mr	: Molecular weight
mRNA	: Messenger ribonucleic acid
MRP1	: Multidrug resistance-associated protein 1
mtDNA	: Mitochondrial DNA
MTT	: 3-(4,5-dimethylthiazol-2-yl)-2,5-diphenyltetrazolium bromide
NADH	: Nicotinamide adenine dinucleotide
NADPH	: Nicotinamide adenine dinucleotide phosphate
Native-PAGE	: Native-polyacrylamide gel electrophoresis
nDNA	: Nuclear DNA
NO	: Nitric oxide
NOS	: Nitric oxide synthase
NO_2^+	: Nitrosonium cation
NPC	: Nasopharyngeal carcinoma
$O_2^{\cdot -}$	: Superoxide radical
O_2^{2-}	: Peroxide
$ONOO^-$	: Peroxynitrite
PDT	: Photodynamic therapy

Q_{10}	: Temperature coefficient
RNS	: Reactive nitrogen species
$RO^{\cdot}$	: Alkoxy
ROO	: Peroxy
ROOH	: Organic hydroperoxide
ROS	: Reactive oxygen species
RSNOs	: S-nitrosothiols
SDS	: Sodium dodecyl sulfate
SDS-PAGE	: Sodium dodecyl sulfate-polyacrylamide gel electrophoresis
Se-H	: Selenol
Se-OH	: Selenenic acid
Se-SG	: Glutathiolated selenol
SOD	: Superoxide dismutase
TEMED	: N, N, N', N'-tetramethylethylenediamine
TRS	: Thiol redox state
Trx	: Thioredoxin
TrxR	: Thioredoxin reductase
V_{max}	: Maximum velocity

LIST OF FIGURES

LIST OF TABLES

1. INTRODUCTION

Human body and other organisms including plants are exposed to oxidative stress which may have exogenous sources such as ultraviolet light, ionizing radiation, environmental toxins, chemotherapeutics and inflammatory cytokines or endogenous sources such as cytochrome p450, mitochondria, peroxisomes, lipoxygenases, photosynthesis and NADPH oxidases. Oxidative stress causes a vital damage to the cell and tissues in all organisms if it is not controlled by antioxidants enzymatically (glutathione reductase, catalase, glutathione peroxidase, glutathione-S-transferase) or non-enzymatically (vitamin C, vitamin D, vitamin E and carotenoids) (Finkel et al., 2000). Since oxidative stress is responsible for the generation of reactive oxygen species (ROS) and reactive nitrogen species (RNS), it induces many chronic diseases including cancer (Valko et al., 2006). It also causes atherosclerosis (Bonomini et al., 2008), diabetes (Asmat et al., 2016), rheumatoid arthritis (Wruck et al., 2011), post-ischemic perfusion injury (Raedschelders et al., 2012), ischemic stroke (Allen and Bayraktutan, 2009), myocardial infarction (Di Filippo et al., 2006), cardiovascular diseases (Dhalla et al., 2000) and chronic inflammation (Khansari et al., 2009).

Glutathione reductase (GR) is a homodimeric FAD-dependent enzyme and belongs to the flavoprotein disulfide oxidoreductase family which participates in the regulation of cellular redox system. The active site of the enzyme contains FAD as a prosthetic group which is reduced by the cofactor NADPH to semiquinone of FAD (a sulfur radical and thiol). Then reduced GR reacts with one molecule of oxidized glutathione (GSSG) leading to the breakdown of disulfide bond which produces a molecule of reduced glutathione (GSH) and GR-SG complex. The second electron from NADPH leads to the breakdown of other disulfide bond in GR-SG complex and second GSH is formed. GR is restored to its oxidizing phase for another enzymatic mechanism (Berkholz et al., 2008). Despite GR is responsible for regeneration of oxidized glutathione, it reduces oxidized glutathione peroxidase to scavenge organic and inorganic peroxides (Igor et al., 2013). Yeast mutant that lack of GR (glr1 delta) showed 200 fold increase in the level of oxidized glutathione which represents 63% of total glutathione. Also in case of mutant thioredoxin (trx1 delta, trx2) high level of oxidized glutathione was observed (Muller, 1996).

Human GR is encoded by a single gene located on chromosome 8p21.1 and composed of 13 exons. GR deficiency is a very rare condition only in case of hemolytic anemia which leads to a decrease or complete absence of the activity of GR (Kamerbeek et al., 2007).

Hypericin is one of the active compounds in St. John's Wort, botanically known as *Hypericum perforatum*. It has come into prominence in the treatment of depression, anxiety, injury of burns and wound-healing. Recent studies recommend an adequacy of this herb in treating different afflictions including cancer, inflammation related disorders, antibacterial and antiviral infections. Hypericin is highly photoreactive, due to its four hydroxyl groups that are situated contiguous two carbonyl groups. In the presence of fluorescent light hydroxyl hydrogen can be transferred between the hydroxyl oxygen and the carbonyl oxygen (Kenneth et al., 2011). Analysis of the fluorescence range of hypericin and its analogs shows the presence of a "protonated" carbonyl group, supporting the H-atom transfer reactions (Petrich, 2000). Hypericin has a strong potential in photodynamic therapy (PDT) because of its photosensitizing effects upon irradiation, minimum toxicity and ability to induce necrosis and apoptosis at very low concentrations in a light dependent manner. It also has role in programmed cell death by promoting several pathways (Agostinis et al., 2002). Inhibition of GR by various compounds have been shown before such as 2-acetylamino-3-[4-(2-acetylamino-2carboxyethylsulfanylthiocarbonylamino) phenylthiocarbamoylsulfanyl] propionic acid (2-AAPA). Although the inhibition of the enzyme was shown, inhibition had no effect on the levels of ROS, GSH biosynthesis enzymes and other antioxidant enzymes, lead to a decline in GSH/GSSG ratio, elevation of $NADH/NAD^+$ and $NADPH/NADP^+$ ratios and an increase in protein glutathionylation. 1,3-bis (2-chloroethyl)-1-nitrosourea (BCNU) is a GR inhibitor. It is used in rabbit lenses in order to indicate the defensive function of GR against oxidative injury. After the lenses were exposed to a constant concentration of H_2O_2, a significant decrease in reduced GSH level was observed.

The aim of this study was to characterize the GR by determining its molecular mass (Mr), pH and temperature optimum. We also tried to elucidate the effect of hypericin on the kinetic behavior of GR purified from baker's yeast.

2. GENERAL INFORMATION

2.1. Glutathione Reductase

Glutathione reductase (GR, E.C. 1.6.4.2), also known as glutathione-disulfide reductase, is a homodimeric flavoprotein enzyme with a molecular weight of 104 kDa. It is found in almost all organisms. It has a main role in producing reduced glutathione (GSH) which has a role in scavenging of free radicals and functions in the cellular control of reactive oxygen species (ROS) that are generated by oxidative stress and xenobiotics, especially in cells with aerobic metabolism. GR, by utilizing NADPH as an electron donor which is generated by pentose phosphate pathway and using FAD as a prosthetic group, produces two reduced glutathione (GSH) molecules from oxidized glutathione (GSSG). GR works parallel with glutathione peroxidase against free radicals and they are the major keys of the antioxidant defense system (Figure 2.1) and inhibition of these antioxidant enzymes causes cell injury and probably death (Tandoğan and Ulusu, 2007).

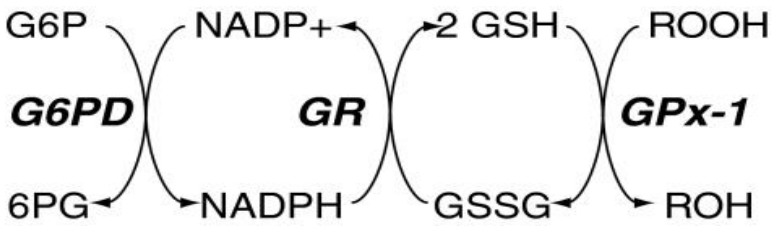

Figure 2.1. Action mechanism of glutathione reductase and glutathione peroxidase. Glutathione reductase (GR) reduces GSSG to GSH by utilizing NADPH that is supplied from pentose phosphate pathway by glucose-6-phosphate dehydrogenase (G6PD) which is necessary to maintain the cofactors for the activation of GPx-1 (Lubos et al., 2011)

Studies showed that inhibition of GR causes a decrease in GSH and increase in GSSG, and ratios of $NADH/NAD^+$ and $NADPH/NADP^+$ increase. On the other hand, inhibition does not influence the development of free radicals and other enzymes of antioxidant defense system (Zhao et al., 2009). Glutathione reductase inhibitors were appeared to have anticancer (Li et al., 2010) and antimalarial actions

(Bauer et al., 2006). The inhibition of GR by Thiram reduces the activity of enzyme and causes a decrease in GSH and accumulation of GSSG (Cereser et al., 2001).

The structure and properties of yeast GR (Glr1) are still under investigation. Yu and Zhou demonstrated the structure of yeast GR by using Pichia pastoris GS115 which was used to allow the expression and recovery of proteins and they compared it with the *E. coli* and *H. sapiens* GRs. Structure of the yeast GR is 50% and 51% similar with *E.coli* and *H. sapiens* enzymes, respectively. They all have three distinct domains, two Rossmann-fold domains (super-secondary structure) for the binding of the FAD prosthetic group and NADPH is the electron donor and the interface domain which is required for dimerization (Figure 2.2). The NADPH-binding domain which thought to be derived from FAD domain by gene duplication and is residing between 198 to 238 residues. Dimerization domain is composed of two parts at the C-terminus from 372 to 483 residues and at the N-terminus from 71 to 104 residues (Yu and Zhou, 2007).

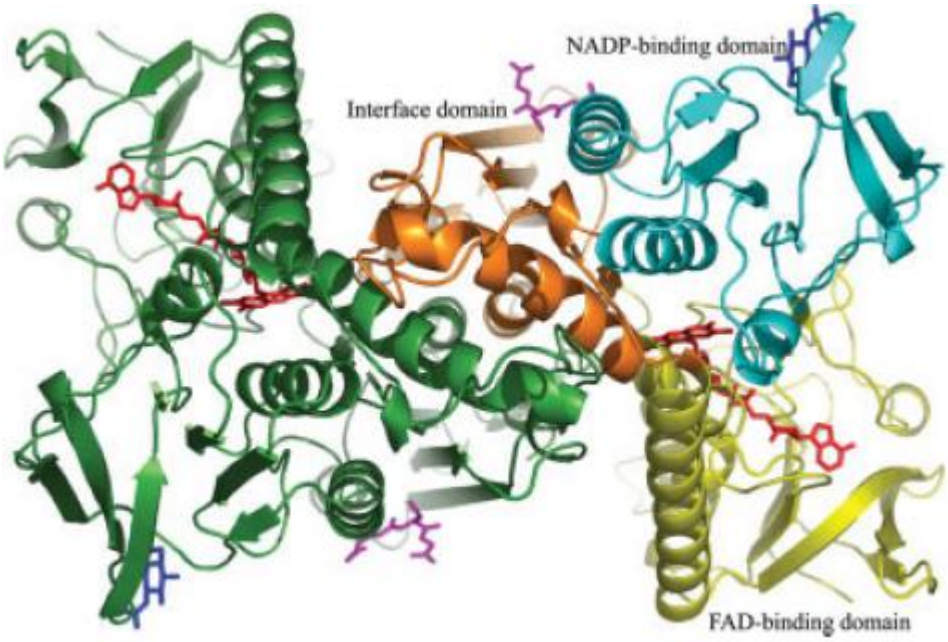

Figure 2.2. Top view of the structure of homodimeric Glr1. Subunit A is colored in dark green. Subunit B represents FAD-binding domain in yellow color, NADPH-binding domain in cyan color. Orange color represents the interface domain. Red and magenta in both subunit's represent FAD and GSH, respectively (Yu and Zhou, 2007).

Studies aimed to demonstrate the catalytic site and the overall mechanism of glutathione reductase revealed that the reaction takes place in two steps. The first step is called reductive half state in which NADPH binds to GR, leading to the reduction of prosthetic group FAD. The reduced flavin then breaks quickly a disulfide bond between Cys_{58}-Cys_{63} forming short living covalent bond with Cys_{63}. This interaction is followed by the charge transfer between flavin and Cys_{63} thiolate and oxidized $NADP^+$ is replaced with the new NADPH. In the second step which is called oxidative half state, Cys_{58} binds to the GSSG and makes a nucleophilic attact to the first cysteine of GSSG and forms a mixed disulfide complex Cys_{58}–GS, leading to a formation of the first reduced glutathione (GSH). After the second GSH is produced, Cys_{58}-Cys_{63} form new disulfide bond and are ready for the reduction of another GSSG (Berkholz et al., 2008) (Figure 2.3).

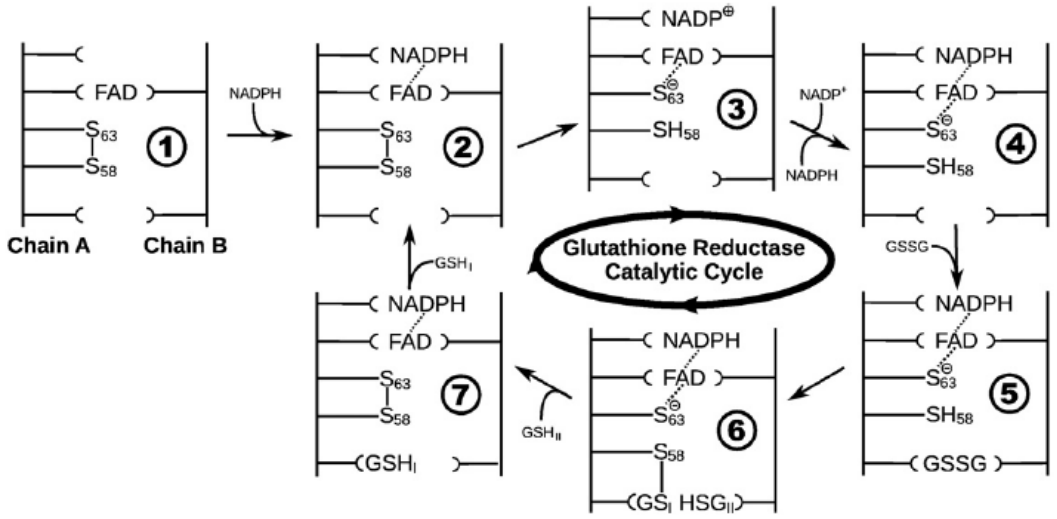

Figure 2.3. Action mechanism of glutathione reductase (Berkholz et al., 2008)

2.2. Glutathione

The tripeptide gamma-glutamyl-cysteinyl-glycine is the most common non-protein thiol peptide in almost all living organisms. It plays important roles in antioxidant defense mechanisms and xenobiotic detoxification because it is a cofactor for several antioxidant enzymes. It also has a role in several cellular processes like DNA and protein synthesis, immune response, signal transduction, cell

proliferation and cytokine production. Glutathione is synthesized by the consequtive action of two cytosolic enzymes, glutamate-cysteine ligase and glutathione synthetase (Figure 2.4). Glutathione synthesis is regulated by the presence of cysteine, glutamate-cysteine ligase activity and also by feedback inhibition of glutathione (Lu, 2013).

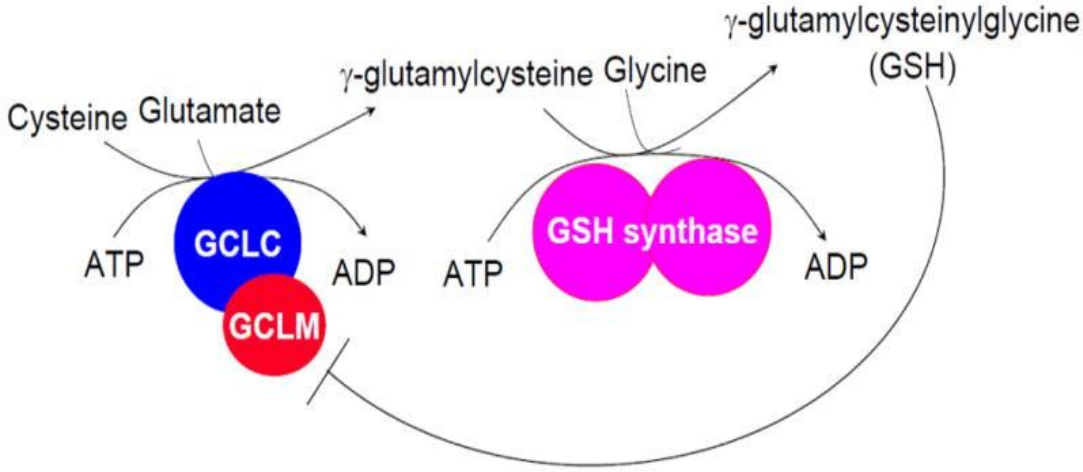

Figure 2.4. Glutathione synthesis (Lu, 2013).

Synthesis of glutathione takes place in two-steps and there is a requirement for ATP. The first step is catalyzed by glutamate-cysteine ligase (GCL), which consists of two subunits, the catalytic (GCLC) and modifier (GCLM) subunits. It integrates cysteine with glutamate, producing γ-glutamylcysteine. The second step is the addition of glycine to γ-glutamylcysteine to form γ-glutamylcysteinylglycine (glutathione) which is catalyzed by glutathione synthetase. Glutathione is the feedback inhibitor of GCL (Lu, 2013).

Glutathione deficiency induces many pathologic diseases including Kwashiorkor (Becker et al., 2005), seizure (Pence et al., 2009), neurodegenerative diseases like Alzheimer's disease (Pocernicha et al., 2012), Parkinson's disease (Smeyne and Smeyne, 2013), cystic fibrosis (Roum et al., 1985), AIDS (Herzenberg et al., 1997), liver disease (Yuan and Kaplowitz, 2009) and sickle cell anemia (Gizi et al., 2011). Studies have shown that glutathione has a crucial effect on lifespan and aging because the concentration of glutathione parallels the telomerase activity (Borrás et al., 2004). The depletion of glutathione leads to the accumulation of

mtDNA damage due to the free radicals and mitochondria loose most of their function (Wei et al., 2001).

2.3. Oxidative Stress

Oxidative stress is an irregularity between the formation of free radicals (reactive oxygen species) and antioxidant defense system (Betteridge, 2000). Reactive oxygen species (ROS) are formed as by-products of natural biological processes during cellular metabolism and additionally, reactive nitrogen species (RNS) that outcome from the cellular redox processes. Free radicals can be characterized as any molecule that contain an unpaired electron in their orbits (Figure 2.5). Most of the radicals are very reactive and unstable. They act as oxidizing or reducing molecules due to their ability to donate or accept an electron from other molecules (Lobo et al., 2010).

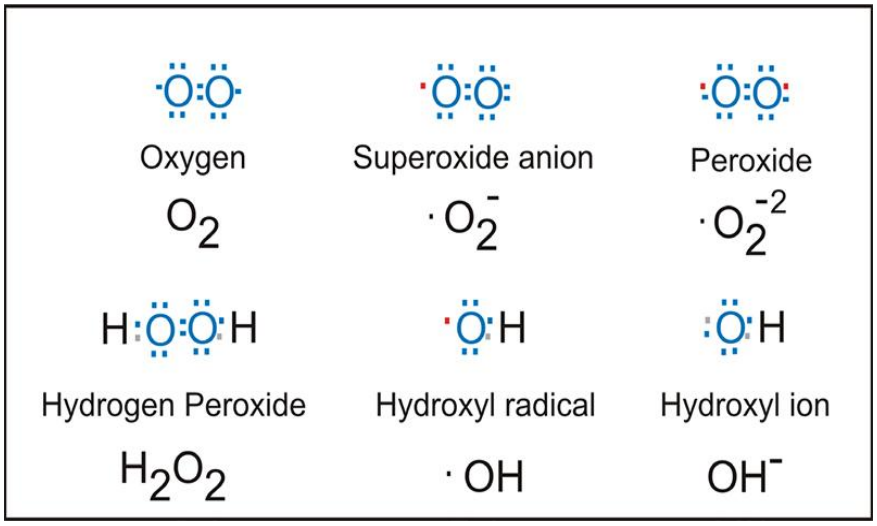

Figure 2.5. Electron structures of common reactive oxygen species. The red • designates unpaired electron.

Oxidants can influence a number of cell signaling pathways and regulate multiple gene expressions in eukaryotic cells. Change in the oxidation-mediated gene expression involves changes in transcription, mRNA stability, flexibility and signal transduction. Moreover, many genes associated with the oxidation products have

been identified, including antioxidant enzymes, stress proteins, DNA repair proteins and proteins of mitochondrial electron transport chain (Powers and Jackson, 2008).

2.3.1. Generation Reactive Oxygen Species in the Human Body

In recent years, there has been a great attention to deal with the field of chemistry of free radicals. They are generated as reactive oxygen species (ROS) and reactive nitrogen species (RNS) by various endogenous systems, exposure to different physical conditions and pathological states. Free radicals and ROS derive either from basic natural metabolic processes in the human body or from external sources such as exposure to UV light irradiation, X-rays, gamma rays, ozone, cigarette smoking, air pollution and industrial chemicals. Continuous formation of free radicals in cells occurs due to both enzymatic and non-enzymatic reactions. Enzymatic reactions, which serve as a source of free radicals include respiratory chain (Cadenas and Davies, 2000), prostaglandin synthesis (Sienko et al., 1991), phagocytosis (Johnston et al., 1975) and cytochrome P-450 system (Dostalek et al., 2008). Free radicals can also be formed in the enzymatic reactions in which molecular oxygen is involved (Lobo et al., 2010).

The generation of ROS can harm multi-organelle cells which could upset inevitably physiology of numerous molecules, for example, lipids, proteins and DNA. Additionally, ROS generation is exhibited in an assortment of diseases, for example, asthma (Henricks and Nijkamp et al., 2001), atherosclerosis (Kisucka et al., 2008), respiratory fibrosis (Bocchino et al., 2010), hypertension (Kitiyakara and Wilcox, 1998), apoptosis (Ott et al., 2007), diabetes retinopathy (Kowluru, 2003) and enactment of proto-oncogenes by starting signal transduction pathways (Korsmeyer et al., 1995) (Figure 2.6). The nature of the injury will ultimately depend on specific molecular interactions, cellular locations, and timing of the insult (Auten and Davis, 2009).

Due to the localization of the mitochondrial electron transport chain for oxygen consuming respiration, mitochondria is a noteworthy hotspot for the generation of ROS. Other mechanisms such as cytoplasmic enzyme systems, the surface of the plasma membrane and endoplasmic reticulum-bound catalysts also contribute to the formation of ROS. Oxygen is a special structure and is fundamental

for the survival of all aerobic organisms. Its two unpaired electrons in separate orbits in the outer electron shell makes oxygen favorable for radical formation by accepting free electrons formed by ordinary oxidative metabolism. Series of sequential steps by the addition of electrons lead to the formation of several ROS including superoxide, hydrogen peroxide and hydroxyl radical (Auten and Davis, 2009) (Figure 2.5).

Figure 2.6. Oxidative stress and related diseases (CC treatment 2015).

Since mitochondria are the principal site for the formation of free radicals, they contain variety of antioxidants which are available on both sides of the membrane to decrease the ROS and minimize oxidative stress (Figure 2.7). For example xanthine oxidase is a form of xanthine oxidoreductase that is capable of the development of superoxide radicals by catalyzing hypoxanthine to xanthine then xanthine to uric acid conversions. During these steps, molecular oxygen is reduced to form superoxide anion and further hydrogen peroxide (Chiricolo et al., 1991). Comparing with nuclear DNA (nDNA), age-related accumulation of oxidative stress markers in mtDNA were detected in human brain. There was a 10 times difference in

the 8-OHdG amount between mtDNA and nDNA. The difference further increased to 15 times when the patients ages were over 70 (Mecocci et al., 1993).

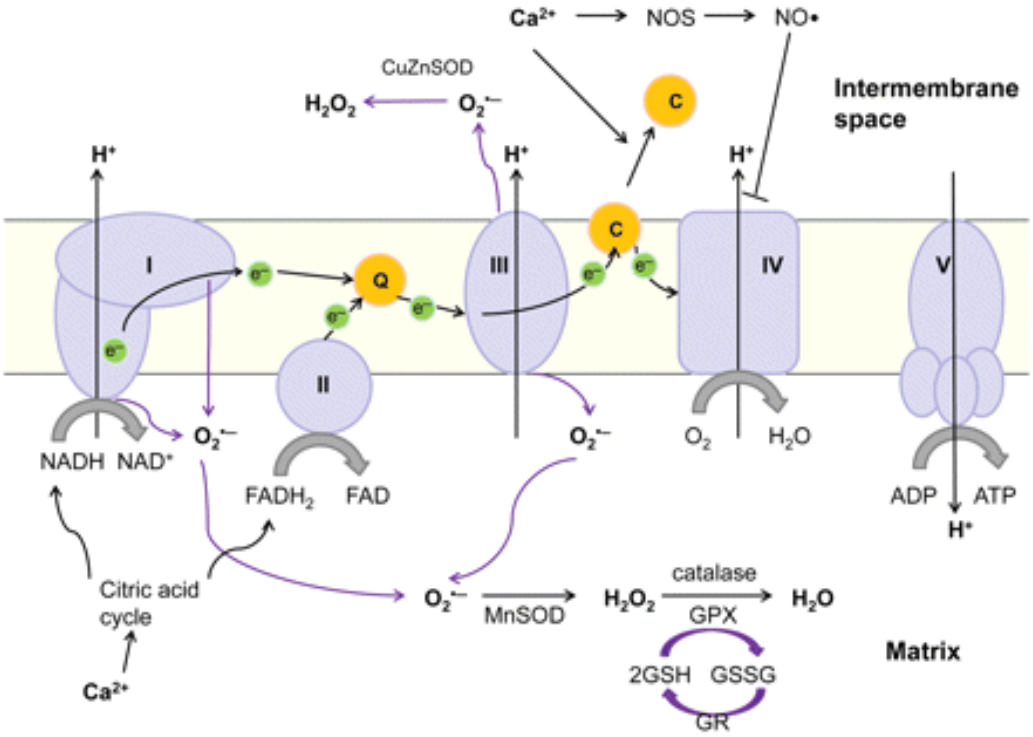

Figure 2.7. Mitochondrial electron transport chain as a main source of free radicals and antioxidant defense systems. When the electrons pass through the complex I and complex III, superoxide ($O_2^{\bullet-}$) radical is produced and it is converted to hydrogen peroxide (H_2O_2) by manganese superoxide dismutase (MnSOD) enzyme located in the mitochondrial matrix or copper zinc superoxide dismutase (CuZnSOD) located in the intermembrane space. Then H_2O_2 is reduced by glutathione peroxidase or catalase enzymes to water. Oxygen molecule is reduced to water as a result of the electron flow through complex IV and by using the proton (H^+) gradient complex V converts ADP to ATP. Ca^{2+} has an influence in generation of ROS by accelerating the Krebs cycle, inducing the loss of cytochrome c and activating nitric oxide synthase (NOS) in turn it inhibits complex IV, resulting the generation of ROS (Yu et al., 2012).

Studies demonstrated that cytochrome p450 enzyme family is a major source for the generation of free radicals due to its important role in metabolism of drugs, xenobiotics, fat-soluble vitamins, carcinogens and eicosanoids (Dostalek et al., 2008). Knockout (CYP2E1-null mice) mice have been developed to understand the role of cytochrome p450s in toxicity and oxidative stress. Administration of analgesic drug acetaminophen to null mice resulted in high level toxicity and elevated production of ROS (Gonzalez, 2005).

Peroxisomes are the other major site of ROS due to their oxygen consuming metabolic processes. Although peroxisomes have a respiratory pathway, it is not coupled to ATP synthesis. Instead transfer of electrons in peroxisomes results in heat production. Peroxisomes also have many enzyme systems that their actions cause the formation of ROS. For example acyl-CoA oxidase, involved in the β-oxidation of fatty acids, whose action leads to the formation of H_2O_2. Since peroxisomes have ROS scavenging enzyme systems, H_2O_2 is reduced to water and oxygen molecules by catalase or by glutathione peroxidase (Schrader and Fahimi, 2006).

2.3.2. Generation of Reactive Nitrogen Species

Reactive nitrogen species (RNS) are a family of molecules derived from nitric oxide (NO) which is a hybrid of nitrogen and oxygen and it has one unpaired electron so it is less reactive than molecular oxygen (Pacher et al., 2007). NO is an intracellular messenger and a physiological regulator of neural and cardiovascular activity. NO is produced from L-arginine by three main isoforms of nitric oxide synthase (NOS) enzyme (Adams et al., 2015). RNS include nitroxyl (HNO), nitrosonium cation (NO^+) and higher oxides of nitrogen, S-nitrosothiols (RSNOs), and dinitrosyl iron complexes (Table 2.1). Interactions of RNS with ROS have been detected in cell injury and death and their potential cellular targets are lipids, DNA and proteins. Harmful effects of RNS depend on their concentration under physiologic conditions (Martínez and Andriantsitohaina, 2009).

Table 2.1. Description of free radicals (Lobo et al., 2010)

Free radicals	**Description**
$O_2^{\cdot -}$ (Superoxide radical)	Produced by addition one electron to O_2. Formed by the electron transport chain and several auto-oxidation reactions. Fe^{2+} from iron-sulfur proteins and ferritin give one electron to O_2 and form superoxide (Fenton recation). It can form H_2O_2 when undergoes dismutation spontaneously or by enzymatic catalysis and is a precursor for metal-catalyzed $OH^{\cdot}$ radical formation.
H_2O_2 (Hydrogen peroxide)	Two-electron reduced state. Formed by dismutation of $O_2^{\cdot -}$ or by direct reduction of O_2. Lipid soluble which is able to diffuse across the membranes.
$OH^{\cdot}$ (Hydroxyl radical)	Three-electron reduction state. Formed by Haber-Weiss reaction and decomposition of peroxynitrite. Very reactive, attack most cellular components.
ROOH Organic hydroperoxide	Produced by radical reactions with cellular components.
$RO^{\cdot}$ Alkoxy ROO Peroxy	Produced in the presence of oxygen by radical addition to double bonds or hydrogen abstraction.
HOCl (Hypochlorous acid)	Formed from H_2O_2 by myeloperoxidase. Lipid soluble and highly reactive. Oxidizes protein molecules including thiol groups, amino groups and methionine.
$ONOO^-$ (Peroxynitrite)	Formed by rapid reaction between $O_2^{\cdot -}$ and NO. Lipid soluble. Protonation forms peroxynitrous acid which undergoes homolytic cleavage to form hydroxyl radical and nitrogen dioxide.

2.3.3. Beneficial Activities of ROS and RNS

Low or moderate concentrations of free radicals are crucial for the several biological processes. They can act as powerful weapons against pathogenic and invading microbes as a defense system of the body (Tatsuzawa et al., 1999) and are regulatory mediators in signaling processes (Droge 2002). Because of its high metabolic activity and high oxygen consumption, brain and neurons are prone to damaging effects of ROS, but at physiological concentration, ROS have a role in maintaining the necessary change in synaptic plasticity and therefore for normal cognitive function (Massaad and Klann, 2011). The immune system produces free radicals as a part of the defense system to protect the body. Phagocytes releases free radicals to eliminate foreign invaders. Patients who suffer from granulomatous diseases are unable to produce superoxide radical ($O_2^{\bullet -}$) because of the defective membrane-bound NADPH oxidase system (Tauber et al., 1983). RNS have physiological roles in the regulation of cellular signaling in various types of nonphagocytic cells including endothelial cells, muscle cells, cardiac myocytes, vascular smooth cells and thyroid tissue fibroblasts. Nitric oxide (NO) is an intercellular messenger that has a role in blood flow, thrombosis and neural activity (Murad, 1996; Pacher et al., 2007; Bryan et al., 2009).

2.4. Antioxidants

Antioxidants which are normally present in low amounts, are molecules capable of donating an electron to stabilize and neutralize free radicals. Human body contains highly complex antioxidant systems (enzymatic and non-enzymatic) which interact easily with the free radicals to scavenge them and protect cells and organs against vital damage. Antioxidants may have exogenous and endogenous sources which means some of the antioxidant molecules can be synthesized during the normal metabolism of the cell such as glutathione and uric acid; others must be provided from dietary supplements (Khalid, 2007). Thus, antioxidants can be divided into three categories: Antioxidant enzymes include catalase (CAT), glutathione peroxidase (GPx), glutathione reductase (GR), superoxide dismutase (SOD) and ceruloplasmin (Figure 2.8); chain breaking antioxidants include lipid phase (tocopherols, ubiquinol, carotenoids and flavonoids) and aqueous phase (ascorbate,

urate, glutathione and other thiols) and transition metal binding proteins include transferrin, ferritin and lactoferrin (Young and Woodside, 2001) (Figure 2.9).

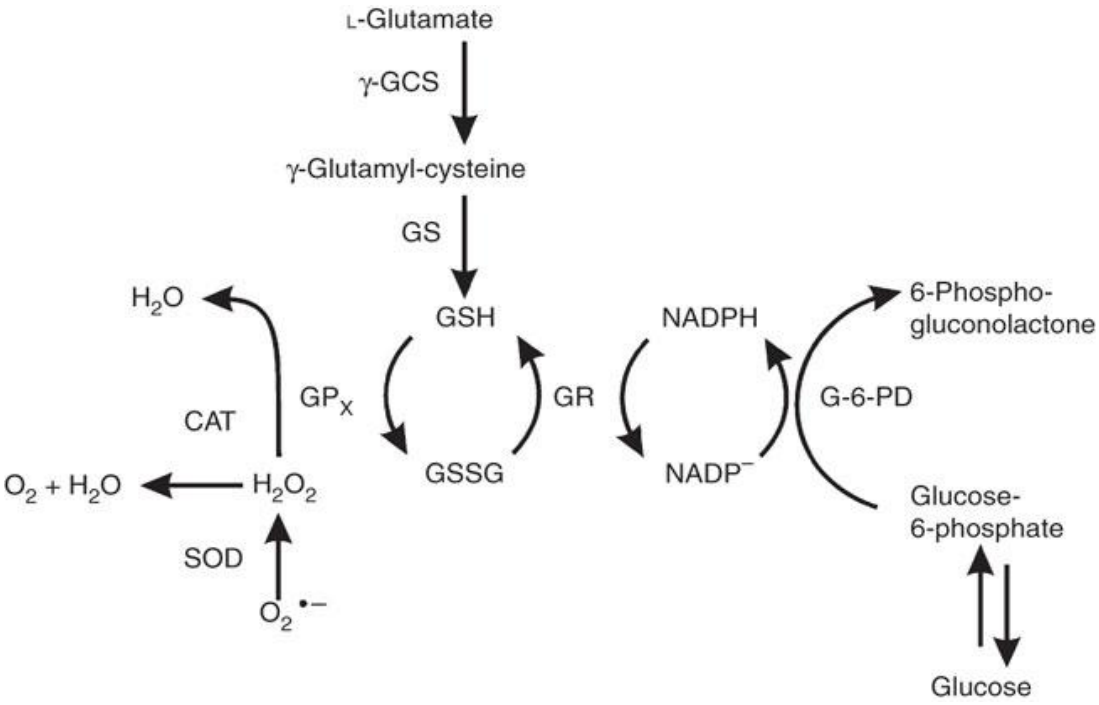

Figure 2.8. The overall antioxidant enzymes, the reactions and detoxification of free radicals (Weydert and Cullen, 2010). Figure illustrates the synthesis of glutathione, formation of NADPH from glucose-6-phosphate by glucose-6-phosphate dehydrogenase, reduction of GSSG to GSH by GR, convertion of $O_2^{\bullet -}$ to H_2O_2 by SOD, reduction of H_2O_2 to water and molecular oxygen by catalase or by GPx.

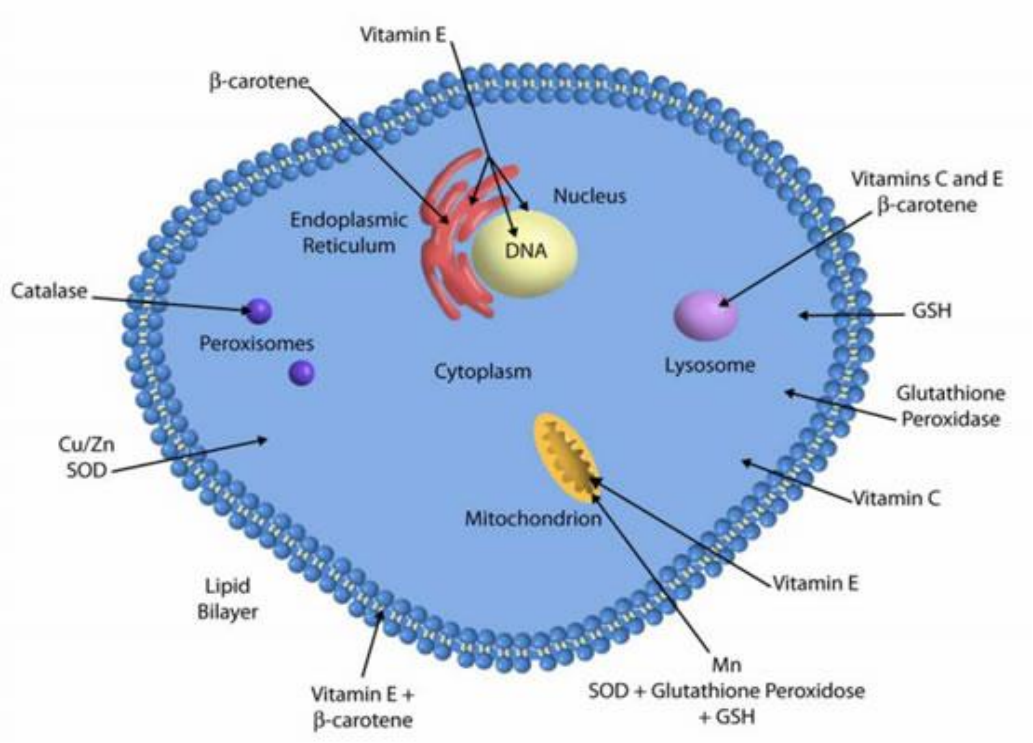

Figure 2.9. Antioxidant systems and their locations (Mandal, 2016)

2.4.1 Antioxidant Enzymes

Catalase

Catalase (CAT) has a role in the regulation of hydrogen peroxide (H_2O_2) metabolism by converting it to water and oxygen molecules. It is found mainly in the peroxisomes of mammalian cells. It is a tetramer of four polypeptide chains, tetrahedrally ordered subunits of 60 kDa. Each subunit has a heme group and NADPH as an electron donor in the active site (Scibior and Czeczot, 2006). Studies showed that CAT has not only a role in decomposition of H_2O_2 to water and oxygen, also at low concentration of H_2O_2 it is responsible for the oxidation of electron donors such as ethanol or phenols (Percy, 1984). Despite the role of CAT on H_2O_2 researchers suggested that CAT has a lower affinity than glutathione peroxidase for H_2O_2. Under physiological conditions detoxification of H_2O_2 occurs by glutathione peroxidase in human erythrocytes (Agar et al., 1986).

CAT reduces H_2O_2 in two steps, first the heme Fe^{3+} reduces a hydrogen peroxide (H_2O_2) to water and produces covalent oxyferryl (Fe^{4+}=O) with a non-

covalent porphyrin π-cation radical, known as compound I. In step two, compound I oxidizes a second peroxide to oxygen and releases the ferryl oxygen species as water (Perry et al., 2007).

$$2H_2O_2 \xrightarrow{\text{Catalase}} 2H_2O + O_2$$

Glutathione Peroxidase

Glutathione peroxidase (GPx) is the most vital enzyme which has a role in the scavenging and detoxifying the peroxides and hydroperoxides to their corresponding alcohols and water as a part of antioxidant defense system (Baker et al., 1993). In mammalian cells there are four GPx's (GPx-1, GPx-2, GPx-3 and GPx-4) which contain selenocysteine at their active sites and there are two others that do not contain selenocysteine (Arthur, 2000). Mills was the first who described GPx in red blood cells with a main function to protect them from hemolysis by oxidation, but now this enzyme is known as GPx-1 which is the most common enzyme in cytosol of mammalian tissues (Mills, 1957). GPx-1 works in parallel with glutathione reductase which keeps up a consistent supply of GSH from GSSG (Arthur, 2000). Studies with the GPx enzyme purified from human plasma demonstrates central beta sheet and many alpha sheets in the structure of the enzyme and selenocysteine is located in the active site between beta 1 and alpha 1 (Ren et al., 1997). The overall reaction shown in Figure 2.10.

In the reaction mechanism, first GPx reacts with peroxide at active site selenol (Se-H) to form a selenenic acid (Se-OH). Selenenic acid is reduced by one molecule of GSH and glutathiolated selenol (Se-SG) intermediate is formed. A second GSH reduces the Se-SG bond and results in the regeneration of the active site with the formation of GSSG (Lubos et al., 2011).

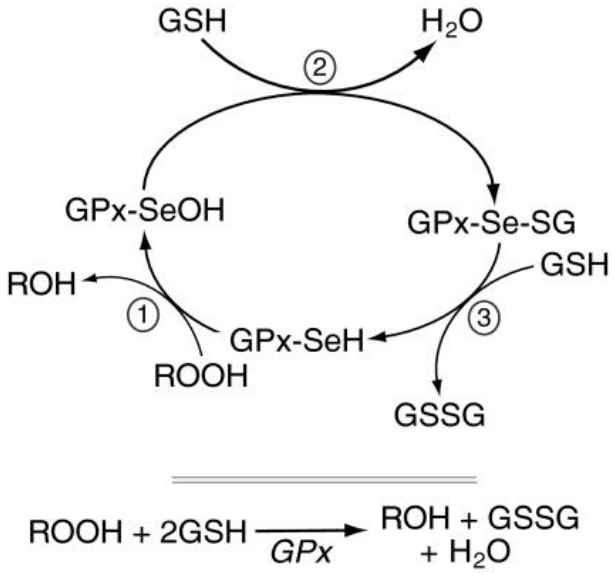

Figure 2.10. Detoxification of peroxides by glutathione peroxidase (Lubos et al., 2011)

Glutathione S-Transferase

Glutathione S-transferases (GSTs) are significant enzymes in phase II detoxification system and found fundamentally in the cytosol of the mammalian cells. GSTs catalyze the conjugation of the tripeptide glutathione (GSH) to an assortment of hydrophobic, electrophilic and generally cytotoxic substrates and have a role in cellular metabolism and detoxification of numerous xenobiotics such as drugs, pollutants and pesticides (Figure 2.11). Mammalian cytosolic GSTs have been classified into eight distinct classes (alpha, mu, pi, theta, kappa, zeta, omega, and sigma) according to their substrate/inhibitor kinetics, structures and immunological similarities (Sheehan et al., 2001; Josephy and David, 2010). Natural hydroperoxides, epoxides, quinones and initiated alkenes are products of oxidative metabolism and they are conceivable "regular" substrates for the GSTs (Mannervik and Danielson, 1988).

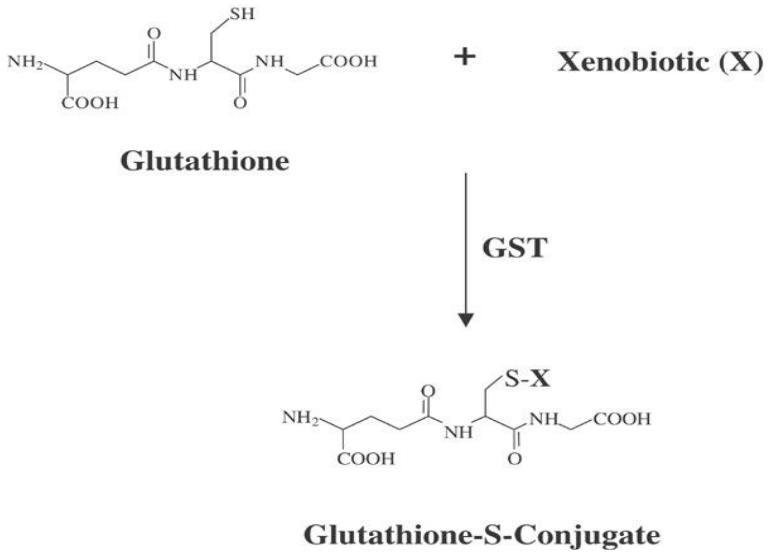

Figure 2.11. Detoxification of xenobiotics by GST. By using the reduced form of glutathione (GSH), GST forms glutathione-S-conjugate via nucleophilic attack which increases the solubility of the conjugate and leads to the elimination of the xenobiotics (Townsend and Tew, 2003).

Superoxide Dismutase

Superoxide dismutase (SOD) is one of the vital antioxidant enzymes which has a crucial role in scavenging of superoxide radical ($O_2\bullet^-$) by converting it to the oxygen molecule and hydrogen peroxide (H_2O_2) with a sole purpose of protecting cells from damage during aerobic respiration (Perry et al., 2007). Mammalian SOD consists of three distinct classes: copper and zinc SOD (Cu/Zn SOD) in cytoplasm, known as SOD1; manganese SOD (Mn-SOD) in mitochondria, known as SOD2 and copper and zinc SOD (Cu/Zn SOD) in extracellular medium, known as SOD3. Mn, Zn and Cu are metals required for their catalytic activities (Fukai and Ushio-Fukai, 2011). In the case of SOD deficiency or inability in other antioxidant mechanisms, the superoxide has many inflicts on pathogenic diseases such as aging, cancer, cardiovascular diseases and neuron abnormalities (Perry et al., 2007). In order to initiate SOD action, active site metals (Cu or Mn) undergo reduction and re-oxidation to scavenge $O_2\bullet^-$ (Figure 2.12).

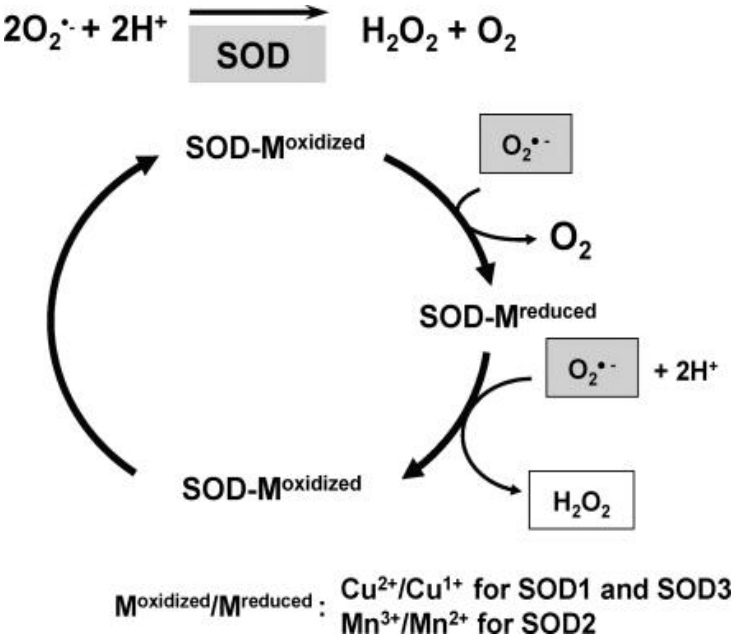

Figure 2.12. Mechanism of SOD in scavenging of superoxide ($O_2•^-$) (Fukai and Ushio-Fukai, 2011)

Thioredoxin Reductases

The thioredoxin reductases (TrxRs) is a homodimeric flavoprotein (10–12 kDa) of pyridine nucleotide-disulphide oxidoreductase family that includes lipoamide dehydrogenase. They have an FAD as prosthetic group and NADPH binding site and an active site with redox-active disulfide. During the reaction one electron is transferred to the active site disulfide from NADPH via FAD (Figure 2.13). Cysteines in the conserved active site peptide (Trp-Cys-Gly-Pro-Cys-Lys) undergo oxidation and reduction. In the reaction mechanism by using the electrons and protons provided by NADPH, thioredoxin (Trx) and/or ascorbate are converted to their reduced forms. Reduced Trx is essential for the activities of Trx peroxidase and ribonucleotide reductase enzymes and transcription factors (Mustacich and Powis, 2000).

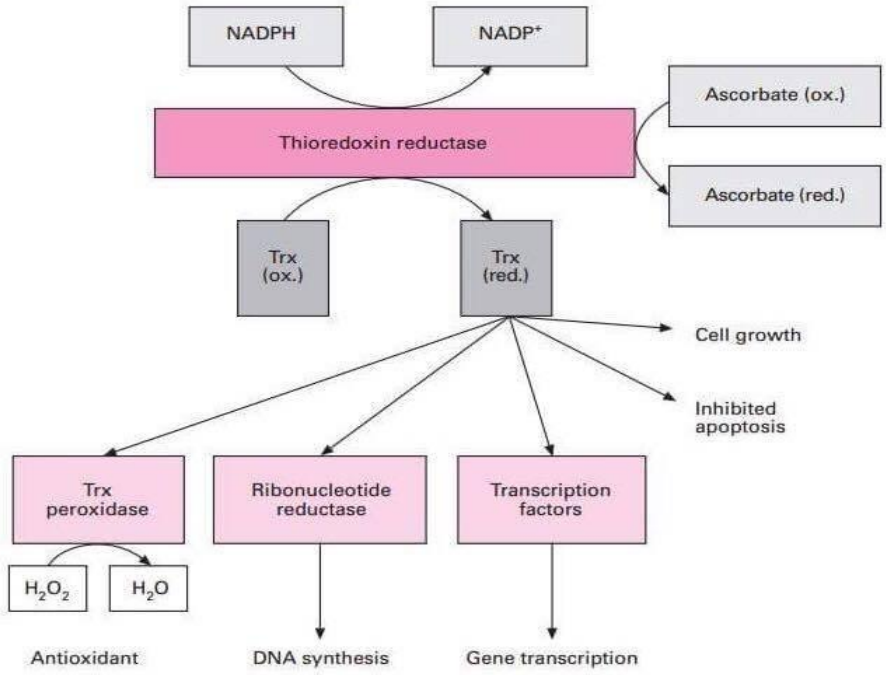

Figure 2.13. Mechanism of action of TrxRs (Mustacich and Powis, 2000)

2.5. Hypericin

Hypericin ($C_{30}H_{16}O_8$) is one of the active ingredient of *Hypericum perforatum* (St. John's Wort). It is a naturally occurring red color pigment with a molecular weight of 504.45 g/mol. It can be also synthesized from anthraquinon emodin (Figure 2.14). It is a multi potential drug in medical application which has an antidepressant, antimicrobial and virostatic effects and is used in photodynamic therapy (PDT) of several oncological (malignant and some non-malignant) diseases. Hypericin inhibits the reuptake of the serotonin, dopamine and norepinephrine in a dose-dependent manner due to its ability to pass through the blood-brain barrier (Assad et al., 2011). It also has an inhibitory effect on various enzymes such protein kinase C (PKC) (Sørensen et al., 2010), NADPH oxidase (Nishiuchi et al., 1995) and TNF-α-induced tyrosyl phosphorylation of neutrophil (Nishiuchi et al., 1995). Recently it has been shown that hypericin decreases the therapeutic availability of some chemotherapeutic drugs like cisplatin and mitoxantrone by increasing the expression of multidrug resistance-associated protein 1 (MRP1) and breast cancer

resistance protein (BCRP), thus it mediates the development of drug resistance (Jendželovská et al., 2014).

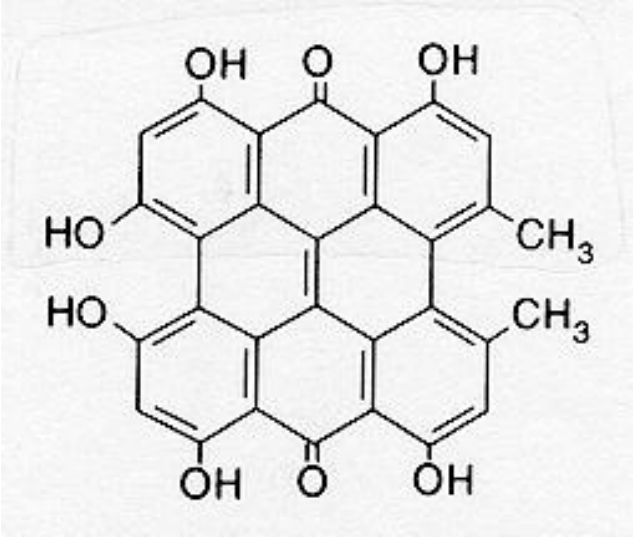

Figure 2.14. Structure of hypericin (Loren, 1999)

Photodynamic therapy (PDT) involves the utilization of photosensitizing agent, which is activated by light with a proper wavelength and further leads to the destruction of the target cell (Abhishek et al., 2012). PDT is initiated by the accumulation of the photosensitizing agent in the hyperproliferative target cells selectively. In the presence of oxygen, local irradiation results in the formation of free radicals. Eventually target cells will die by apoptosis or necrosis (Luksiene, 2003; Maduray and Davids, 2011). Hypericin is a selective anti-cancer photosensitizing agent with high photon yield without any toxic effects (Barathan et al., 2013). Photodynamic therapy with hypericin induces apoptosis in human umbilical vein endothelial cells in the presence of molecular oxygen which is required to generate ROS (Zhang et al., 2015). *In vitro* testing of hypericin in squamous cell carcinoma revealed that hypericin is useful in PDT when it is used in 0.2–0.5 μg/ml concentration range and 593 nm laser light irradiation is applied (Head et al., 2006). *In vivo* hypericin administration with laser phototherapy has role in decreasing pancreatic cancer growth (Kwan et al., 2000). Also hypericin controls tumor cell growth in nasopharyngeal carcinoma (NPC) *in vivo* (Yee et al., 2005).

3. MATERIALS AND METHODS

3.1. Chemicals

Potassium phosphate (monobasic and dibasic), Reduced nicotinamide adenine dinucleotide phosphate (NADPH), trizma base, ammonium persulfate, silver nitrate, formaldehyde, dichlorophenol indophenol, 2-mercaptoethanol, glycerol, bovine serum albumin, bromophenol blue, N,N'-methylenebisacrylamide, glutathione reductase from baker's yeast, N,N,N',N'-tetramethylethylenediamine, Glycine ,Acrylamide, Ethanol, methanol, sodiumthiosulfate, sodium azide, sodium carbonate, dimethyl sulphoxide (DMSO) and 3-(4,5-dimethylthiazol-2-yl)-2,5-diphenyltetrazolium bromide (MTT) were purchased from sigma Aldrich (St. Louis, MO, USA). Coomassie Brilliant Blue R-250 and Coomassie Brilliant Blue G-250 were procured from Fluka (Steinhein, Germany). Oxidized glutathione was taken from Fluka (Switzerland). Acetic acid and ethanol were obtained from Riedel-de Haën (Germany). Orthophosphoric acid is acquired from Applichem (Darmstadt Germany). Roti-mark standard was obtained from Carl Roth GmbH (Karlsruhe, Germany). Hypericin was purchased from Alexis Biochemical (Lausen, Switzerland).

3.2. Methods

3.2.1. Preparation of Glutathione Reductase

Baker's yeast glutathione reductase (GR) was procured from Sigma Aldrich (St. Louis, MO, USA). Enzyme suspension contained 3.6 M ammonium sulfate and 0.1 M dithiothreitol. Enzyme was centrifuged at 20800 xg for 20 minutes at 4^{o}C in order to remove ammonium sulfate. After centrifugation, supernatant was separated, pellet was dissolved in 20 mM phosphate buffer pH 7.4 and used in the experiments.

3.2.2. Determination of Protein Concentration by Bradford Assay

Bradford assay is the most common method used to determine the protein concentration (Bradford, 1976). The Coomassie Brilliant Blue G-250 is acidic dye which specifically binds basic amino acids (histidine, lysine and arginine). Upon formation of dye-protein complex the wavelength shifts from 470 nm to 595 nm.

Bradford reagent was prepared as follows: Coomassie Brilliant Blue G-250 (25 mg) was was mixed with 12.5 ml of absolute ethanol in order to dissolve the dye. Then 25 ml of 85% of orthophosphoric acid was added and final volume was brought to 250 ml with distilled water. The reagent was filtered by Whatman No: 1 filter paper and stored in dark at room temperature.

As a standard bovine serum albumin (BSA) was used. Six different BSA concentrations (50 µg/ml, 100 µg/ml, 200 µg/ml, 300 µg/ml, 400 µg/ml and 500 µg/ml) were prepared by diluting 1 mg/ml of stock BSA solution. Twenty µl of standard BSA solutions and samples were mixed with 1 ml of Bradford reagent. After keeping all the samples at dark for 5 min at room temperature, absorbances of standards and samples were measured at 595 nm by using Perkin Elmer Lambda 25 UV/VIS Spectrophotometer (Perkin Elmer, Singapore). The standards and samples were prepared in triplicates. Concentration of GR was determined by using standard curve.

3.2.3. Native-Polyacrylamide Gel Electrophoresis (Native-PAGE)

Purity of GR was confirmed by discontinuous native-PAGE (Hames, 1998). Coomassie Brilliant Blue (CBB) R-250, silver and activity stainings were performed to visualize protein and activity bands. The final concentrations of gels to be used in CBB and silver stainings were 6% for separating gel and 4% for stacking gel. For activity staining, separating and stacking gels were prepared as 10% and 4%, respectively.

Reagents used in Discontinuous Native-PAGE

- 30% Acrylamide/Bisacrylamide solution (29.4% acrylamide/0.6% N,N-methylenebisacrylamide)
- Separating gel buffer: 1.5 M Tris/HCl, pH 8.8
- Stacking gel buffer: 0.5 M Tris/HCl, pH 6.8
- 10x Electrode (running) buffer: 25 mM Tris (Base), 192 mM glycine
- 2x Sample buffer: 1.25 ml of 0.5 M Tris/HCL pH 6.8, 4 ml glycerol, 10 mg bromophenol blue and the volume was adjusted to 10 ml with distilled water.
- 10% ammonium persulfate (APS), prepared daily
- N,N,N,’N’-tetramethylethylenediamine (TEMED)

Preparation of Gel for Native-PAGE

The spacer (1.5 mm) and the plain glasses were placed vertically on the casting stand. The separating gel mixture (6.5 ml) was loaded into the plain glasses and distilled water was layered on in order to have a smooth surface. Gel was left for about 1 hour for polymerization. After polymerization of the separating gel, layered water is discarded. Stacking gel mixture was added onto separating gel and the 10 well comb was immediately placed in the gel and kept for about 1 hour 30 minutes for complete polymerization. The plain glasses were removed from the casting stand and placed in the electrophoresis assembly and transferred into the electrophoresis tank. Tank was filled with running buffer and the 10 well combs were removed. Before loading the samples into the wells, the wells were washed with the running buffer solution.

Table 3.1. Volumes used in gel preparation of Native-PAGE

	Separating Gel (6% or 10%)	Stacking gel (4%)
30% Acrylamide / Bisacrylamide	3 ml (for 6%) 5 ml (for 10%)	1.33 ml
1.5 M Tris/HCL, pH 8.8	3.75 ml	-
0.5 M Tris/HCL, pH 6.8	-	2.5 ml
Distilled water	8.25 ml (for 6%) 6.17 ml (for 10%)	6.12 ml
10% APS	75 µl	40 µl
TEMED	7.5 µl	10 µl
Total Volume	15 ml	10 ml

Sample Preparation for Native-PAGE

Three different sample preparation methods were employed according to the staining method. First, the reducing agent, 2-mercaptoethanol (2-ME) was diluted 100 times. To the stock enzyme (15 µl) 1.13 µl of diluted 2-ME is added and incubated for 1 hr at room temperature. Final enzyme concentration in each well was adjusted to 5 µg, 3.75 µg, 2.5 µg and 1.25 µg for CBB staining; 0.5 µg, 0.375 µg, 0.25 µg and 0.125 µg for silver staining and 4 µg, 8 µg and 12 µg for activity staining.

- **Sample preparation for CBB staining**

1. 1 µl of stock enzyme + 3.8 µl of 20 mM phosphate buffer pH 7.4
2. 1 µl of stock enzyme + 5.4 µl of 20 mM phosphate buffer pH 7.4
3. 1 µl of stock enzyme + 8.6 µl of 20 mM phosphate buffer pH 7.4
4. 1 µl of stock enzyme + 18.2 µl of 20 mM phosphate buffer pH 7.4

Sample was mixed with sample loading buffer at 1:1 ratio just before the application into the gel, 20 µl of sample was loaded into the wells.

- **Sample preparation for silver staining**

First the enzyme was diluted 10 times.

1. 4 µl of diluted enzyme + 15.2 µl 20 mM phosphate buffer pH 7.4
2. 3 µl of diluted enzyme + 16.2 µl 20 mM phosphate buffer pH 7.4
3. 2 µl of diluted enzyme + 17.2 µl 20 mM phosphate buffer pH 7.4
4. 1 µl of diluted enzyme + 18.2 µl 20 mM phosphate buffer pH 7.4

Sample was mixed with sample loading buffer at 1:1 ratio just before the application into the gel, 20 µl of sample was loaded into the wells.

- **Sample preparation for activity staining**

1. 10 µl of stock enzyme + 20 µl dH_20 + 10 µl sample loading buffer
2. 20 µl of stock enzyme + 10 µl dH_20 + 10 µl sample loading buffer
3. 30 µl of stock enzyme + 10 µl sample loading buffer

Twenty µl of sample was loaded into the wells.

Bio-Rad Miniprotean Tetra Cell electrophoresis system was used. Electrophoresis was initiated with 120V and when the samples migrated into the separating gel, the voltage was increased to 150 V. Electrophoresis was completed when the bromophenol blue dye reached about 1 cm to the end of the gel. Gels were transferred into petri dishes for staining processes.

3.2.4. Sodium Dodecyl Sulfate-Polyacrylamide Gel Electrophoresis (SDS-PAGE)

Purity and relative molecular weight (M_r) of GR were confirmed by SDS-PAGE. Concentrations of separating and stacking gels were 7% and 4%, respectively (Laemmli, 1970).

Reagents used in discontinuous SDS-PAGE

- 30% Acrylamide/Bisacrylamide solution (29.4% acrylamide/0.6% N,N-methylenebisacrylamide)
- Separating gel buffer: 1.5 M Tris/HCl, pH 8.8
- Stacking gel buffer: 0.5 M Tris/HCl, pH 6.8
- 5x Electrode (running) buffer pH 8.3 was taken from already prepared native gel running buffer (10 x) containing 15g/L Tris Base and glycine 72 g/L. To the 5x electrode buffer, 6 gr of SDS was added.
- 2x Sample buffer: 3 ml 1.5 M Tris pH 6.8, 5 gr glycerol i.e 4 ml, 1.6 ml of BPB, 2.8 µl of β-ME (added immediately during sample preparation), 0.37 ml of dH_2O, 1 ml of 10% SDS
- 10% SDS solution
- 10% ammonium persulfate (APS), prepared daily.
- N,N,N,'N'-tetramethylethylenediamine (TEMED)

Preparation of Gel for SDS-PAGE

The spacer (1.5 mm) and the plain glasses were placed vertically on the casting stand. The separation gel mixture (6.5 ml) was loaded into the plain glasses and distilled water was layered in order to have a smooth surface. The gel was left for about 1 hour for polymerization. After polymerization of the separating gel,

layered water is discarded. Stacking gel was also added onto the separating gel and the 10 well comb was immediately placed in the gel and kept for about 1 hour 30 minutes for complete polymerization. The plain glasses were removed from the casting stand and placed in the electrophoresis assembly and transferred into the electrophoresis tank. Tank was filled with running buffer containing SDS and the 10 well combs were removed. Before loading the samples, wells were washed with the running buffer solution.

Table 3.2. Volumes Used in Gel Preparation of SDS-PAGE

	Separating Gel (7%)	Stacking Gel (4%)
30% Acrylamide/Bisacrylamide	3.5 ml	1.33 ml
1.5 M Tris/HCL, pH 8.8	3.75 ml	-
0.5 M Tris/HCL, pH 6.8	-	2.5 ml
Distilled water	7.57 ml	6.07 ml
10% SDS	100 µl	100 µl
10% APS	75 µl	50 µl
TEMED	7.5 µl	10 µl
Total Volume	15 ml	10 ml

Sample Preparation for SDS-PAGE

According to the staining method, sample was prepared in two different ways. Final enzyme concentration in each well for CBB staining was adjusted to 4 µg, 8 µg and 12 µg. For silver staining, enzyme concentrations were 0.4 µg, 0.8 µg and 1.2 µg. Roti-mark protein molecular weight marker was used.

- **Sample preparation for CBB staining**

1. 10 µl of stock enzyme + 20 µl of dH_2O + 10 µl of sample loading buffer
2. 20 µl of stock enzyme + 10 µl of dH_2O + 10 µl of sample loading buffer
3. 30 µl of stock enzyme + 10 µl of sample loading buffer

Samples were incubated at 95^{o}C for 3 min and 20 µl of sample was loaded into the wells.

- **Sample preparation for silver staining**

1. 1 µl of stock enzyme + 29 µl of dH_2O + 10 µl of sample loading buffer
2. 2 µl of stock enzyme + 28 µl of dH_2O + 10 µl of sample loading buffer
3. 3 µl of stock enzyme + 27 µl of dH_2O + 10 µl of sample loading buffer

Samples were incubated at 95^{o}C for 3 min and 20 µl of sample was loaded into the wells.

Bio-Rad Miniprotean Tetra Cell electrophoresis system was used. Electrophoresis was initiated with 150 V and when the samples migrated into the separating gel, the voltage was increased to 200 V. Electrophoresis was completed when the bromophenol blue dye reached about 1 cm to the end of the gel. Gels were transferred into petri dishes for staining processes.

3.2.5. Coomassie Brilliant Blue (CBB) R-250 Staining

After native and SDS-PAGE, CBB staining protocol was carried out in order to visualize the protein bands on the gel. Staining solution was prepared from 0.1% Coomassie Brilliant Blue R-250, 40% methanol and 10% acetic acid. After native and SDS-PAGE, gels were incubated with the staining solution for 30 minutes or overnight and then transferred into destaining solution. The destaining solution was consist of 40% methanol and 10% acetic acid. Destaining solution was replaced every 30 minutes till the background was clear. Then gels were stored in 5% acetic acid at 4^{o}C (Wilson et al., 1979).

3.2.6. Silver Staining

Upon completing the native and SDS-PAGE, silver staining was carried out according to the method described by Blum et al. with slight modifications (Blum et al., 1987). Gels were fixed with 50% methanol, 12% glacial acetic acid and 0.005% formalin solution for 2 hours or overnight. Then the fixation solution was discarded and gels were washed three times with 50% ethanol for 20 minutes. Gels were sensitized with 0.02% sodium thiosulfate ($Na_2S_2O_3$) for 2 minutes and then washed

with distilled water three times for 20 seconds. Gels were stained with 0.2% silver nitrate ($AgNO_3$) and 0.076% formalin solution for 20 minutes. After staining, gels were washed with distilled water twice for 20 seconds. Gels were kept in 6% sodium carbonate (Na_2CO_3), 0.05 formalin and 0.0004% sodium thiosulfate solution until the bands were visible. When the bands were clearly seen, gels were washed with distilled water twice for 2 minutes. Staining was finalized by the addition of a stop solution which was made up of 40% methanol, 10% glacial acetic acid and gels were embedded in this solution for 20 minutes. After completion of the staining procedure, gels were stored in 1% glacial acetic acid solution at 4^oC.

3.2.7. Activity Staining

After native-PAGE was carried out, activity staining procedure of Graubaum on cellulose acetate was modified and applied to native-PAGE (Graubaum, 1981). Three different solutions were used for activity staining. Gel was first incubated in 15 ml of 100 mM potassium phosphate buffer pH 7.5 for 2 minutes. Then, gel was incubated in 100 mM potassium phosphate buffer pH 7.5 containing 1.0 mg MTT, 0.100 mg of dichlorophenol indophenol for 10 minutes. Finally, gel was incubated in 100 mM potassium phosphate buffer pH 7.5 containing 2.5 mg NADPH and 18 mg GSSG until color developed.

3.2.8. Glutathione Reductase Activity Measurement

Glutathione reductase activity was measured according to method of Carlberg and Mannervik by using Perkin Elmer Lambda 25 UV/VIS Spectrophotometer (Carlberg and Mannervik, 1985). The reaction mixture contained 100 mM potassium phosphate buffer pH 7.4, 1 mM GSSG, 0.1 mM NADPH and 25 µl of enzyme. GR was added last to initiate the reaction. Increase in the absorbance at 340 nm was followed for 30 seconds at 37°C. Each activity measurement was repeated in triplicates. Average activity (U/L) values were converted to specific activity (U/mg protein) and specific activity values were used to draw the following plots: Optimum temperature, Michaelis-Menten, Lineweaver-Burke and Dixon (Segel, 1975).

$$\text{Specific Activity (Unit/mg protein)} = \frac{\Delta Abs_{340} \times V_t \times 1000}{6.22 \times V_s \times [\text{Protein}]}$$

ΔAbs_{340}/min : Absorbance change per minute at 340 nm

V_t : Volume of total activity measurement mixture (500 µl)

V_s : Enzyme volume (µl) used in the measurement of enzyme activity

6.22 : Extinction coefficient of NADPH (mM)

1000 : A factor used to convert ml to liter

Kinetic parameters for GR were determined by using variable concentrations of GSSG (0.0625 mM, 0.125 mM, 0.25 mM, 0.5 mM and 1 mM) while keeping the NADPH concentration constant (0.1 mM) and also by using variable concentrations of NADPH (0.01 mM, 0.015 mM, 0.02 mM, 0.04 mM and 0.1 mM) while keeping GSSG concentration constant (1 mM) (Carlberg and Mannervik, 1985).

3.2.9. Determination of Optimum pH by Zero Buffer Extrapolation

To determine the pH optimum of GR, "zero buffer extrapolation" was carried out in order to eliminate the effect of potassium phosphate buffer on enzyme activity. The activity measurements were carried out in phosphate buffers at different pH values (6, 6.5, 7, 7.5, 8, 8.5, 9) and at different concentrations (50 mM, 100 mM, 150 mM, 200 mM). From the activity versus buffer concentration graph the activities at zero buffer were determined by extrapolation and the activity at zero buffer concentration versus pH graph was performed. From the second graph the pH optimum for GR was found. Final GSSG and NADPH concentrations were 1 mM and 0.1 mM, respectively. Each pH value and buffer concentration was tested three times at 37°C and the reaction was monitored at 340 nm for 30 seconds. Average ΔA/min was calculated for each pH value.

3.2.10. Determination of Optimum Temperature

Activity measurement of the glutathione reductase enzyme was performed at different temperature values to determine the effect of temperature on enzyme

activity. Reaction mixture contained 100 mM potassium phosphate buffer pH 7.5, 1 mM GSSG, 0.1 mM NADPH and 25 µl of glutathione reductase enzyme. Temperature of the reaction medium was adjusted to certain points (20°C, 25°C, 30°C, 35°C, 40°C, 45°C, 50°C, 55°C, 60°C, 65°C, and 70°C) by using water bath. The reaction was monitored at 340 nm for 30 sec. Each temperature point was tested three times. Average specific activity was calculated and used to draw graphics (Carlberg and Mannervik, 1985).

3.2.11. Effect of Hypericin on Glutathione Reductase Enzyme Activity

Hypericin was dissolved in dimethyl sulphoxide (DMSO). Reaction mixture consisted of 100 mM potassium phosphate buffer pH 7.5, 1 mM GSSG, 0.1 mM NADPH, 25 µl of GR and 10 µl of hypericin prepared in different concentrations (1.5625 µM, 3.1275 µM, 6.25 µM, 12.5 µM, 25 µM, 50 µM and 100 µM). Enzyme activity for each hypericin concentration was measured at 340 nm for 30 seconds at 37^{o}C (Carlberg and Mannervik, 1985). Each activity measurement was performed in triplicates. Average specific activity was calculated and used to draw related graphics.

3.2.12. Inhibitory Kinetic Experiments with Hypericin

Kinetic studies were carried out to determine K_m and V_{max} values for glutathione reductase enzyme in the presence of variable hypericin concentrations. Four hypericin concentrations (1 µM, 2 µM, 4 µM and 8 µM) were tested while [GSSG] (0.03125 mM, 0.0625 mM, 0.125 mM, 0.25 mM, 0.5 mM and 1mM) and [NADPH] (0.01 mM, 0.015 mM, 0.02 mM, 0.04 mM and 0.1 mM) were the variable substrates. First the activity of the enzyme was tested with variable hypericin and GSSG concentrations at constant [NADPH] (0.1 mM). Then by using same hypericin concentrations, activity measurements were performed with variable [NADPH] and constant [GSSG] (1 mM). Each measurement was repeated three times. Decrease in absorbance at 340 nm was monitored for 30 seconds at 37^{o}C (Carlberg and Mannervik, 1985). Average specific activity was calculated and used to related draw graphics.

3.3.13. Statistical Analysis

SPSS version 22 was used in the estimation of inhibition type and calculation of kinetic parameters.

4. RESULTS

4.1. Determination of the Protein Concentration

Glutathione reductase purified from baker's yeast was purchased from Sigma Aldrich and used in further experiments. The protein concentration was determined by Bradford assay (Bradford, 1976). Bovine serum albumin (BSA) was used as a standard with final concentrations of 50 µg, 100 µg, 200 µg, 300 µg, 400 µg and 500 µg. Samples (20 µl) were mixed with 1 ml of Bradford reagent, followed by 5 min incubation at dark and the absorbances of standards and samples were read at 595 nm. Protein concentration of GR was determined from the standard curve (Figure 4.1).

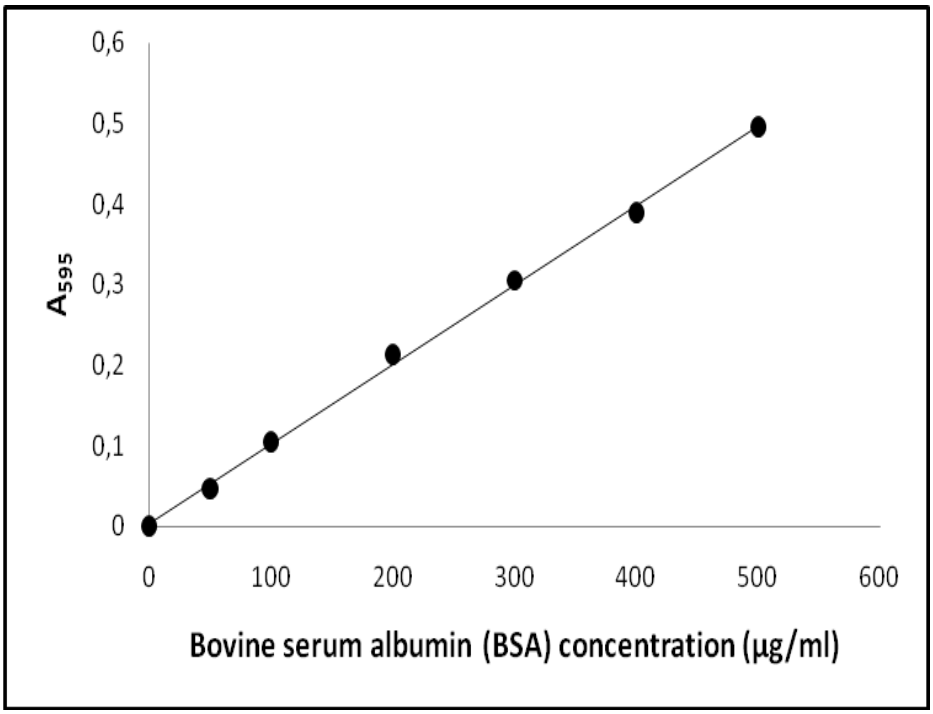

Figure 4.1. Determination of the enzyme concentration by Bradford assay

Glutathione reductase was separated from its solvent ammonium sulphate ($AmSO_4$) and thereafter dissolved in 20 mM potassium phosphate buffer pH 7.4. The enzyme concentration was calculated as 813 µg/ml.

4.2. Characterization of Glutathione Reductase Enzyme

4.2.1. Purity Control of Glutathione Reductase Enzyme

Determination of the purity and molecular weight of the GR enzyme was carried out by native and SDS-PAGE. Coomassie Brilliant Blue R-250, silver and activity stainings were performed in order to visualize protein bands. In native gel, purity of the enzyme was confirmed by the visualization of a single protein band after CBB (Figure 4.2.A), activity (Figure 4.2.B) and silver stainings (Figure 4.3).

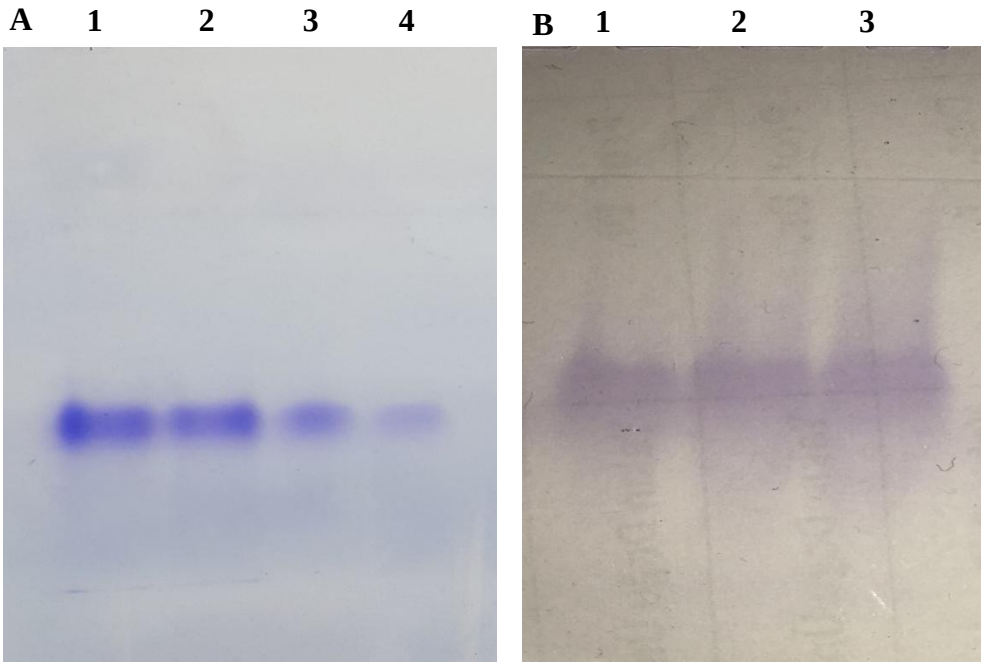

Figure 4.2. Visualization of GR enzyme on discontinuous native-PAGE. A. Coomassie Brilliant Blue G-250 staining of glutathione reductase. Separating and stacking gels were prepared 6% and 4%, respectively. Protein concentration in lane 1, 5 μg; lane 2, 3.75 μg; lane 3, 2.5 μg; lane 4, 1.25 μg. B. Activity staining of glutathione reductase. Separating and stacking gels were prepared 10% and 4%, respectively. Protein concentration in lane 1, 4 μg; lane 2, 8 μg; lane 3, 12 μg.

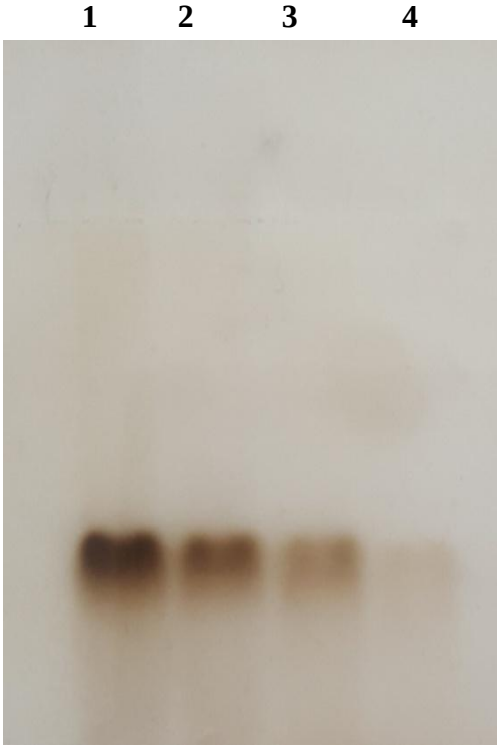

Figure 4.3. Visualization of GR enzyme on discontinouse native-PAGE by silver staining. Separating and stacking gels were prepared 6% and 4%, respectively. Protein concentration in lane 1, 0.5 µg; lane 2, 0.375 µg; lane 3, 0.25 µg; lane 4, 0.125 µg.

Subunit molecular weight of the GR was determined by SDS-PAGE. Protein band belongs to the subunits of the GR was identified in gels stained with both CBB (Figure 4.4A) and silver staining (Figure 4.5). Molecular weight of each subunit was calculated as 49 kDa by using molecular weight marker proteins and their migration distances (Figure 4.4.B).

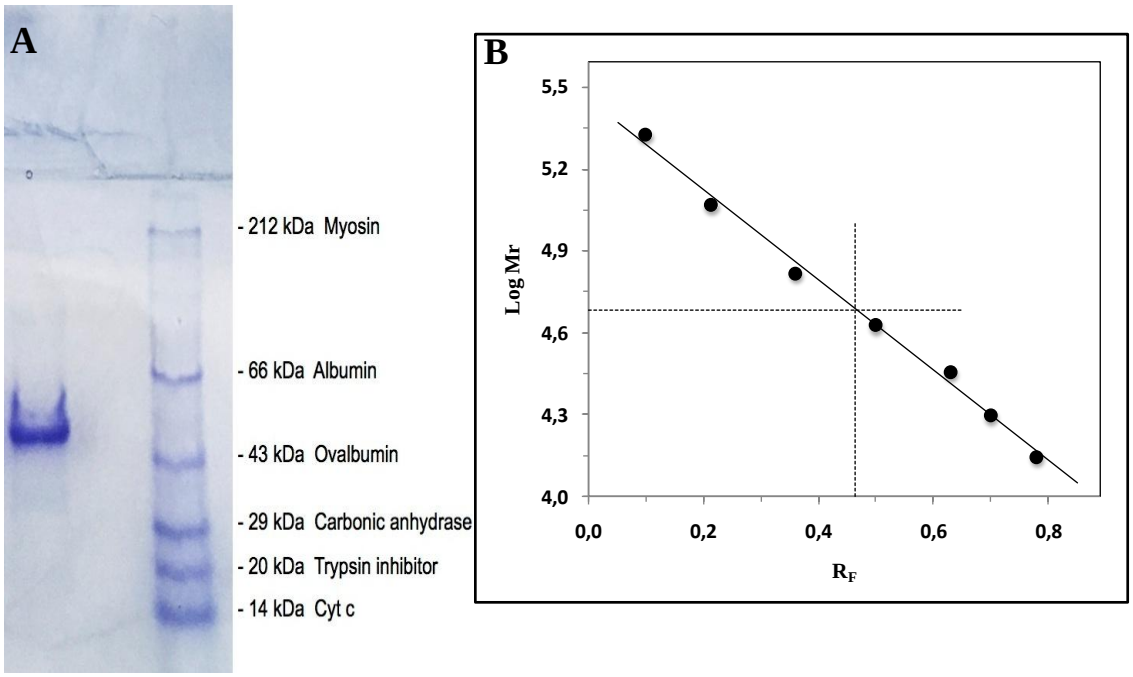

Figure 4.4.A. Glutathione reductase enzyme on discontinuous SDS-PAGE by Coomassie Brilliant Blue R-250 staining. Separating and stacking gels were prepared 7% and 4% respectively. Concentration of glutathione reductase enzyme was 4µg. Figure 4.4.B. Log M_r vs R_f plot.

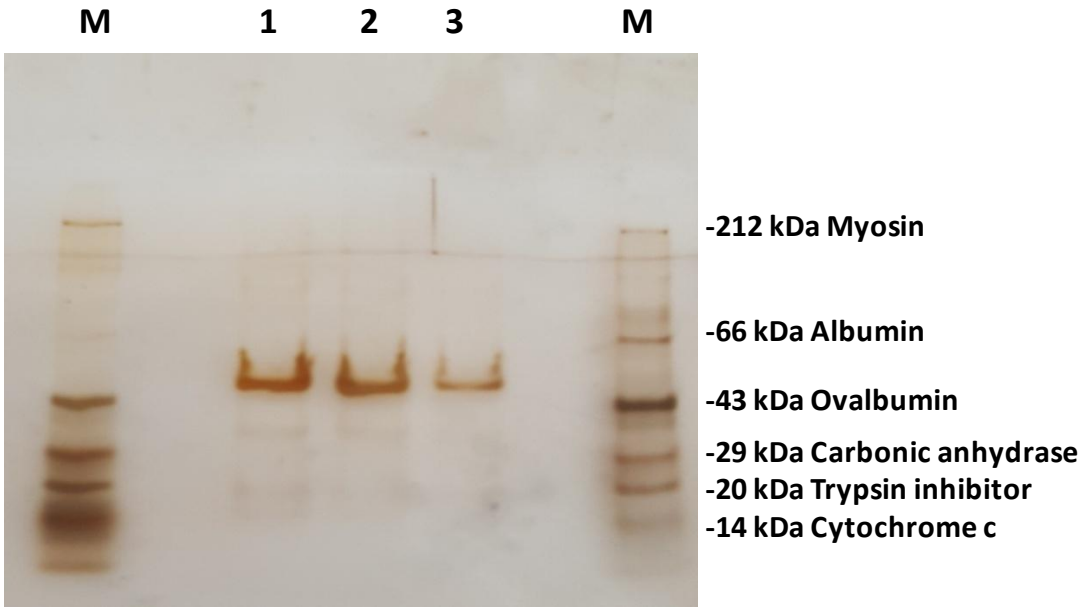

Figure 4.5. Glutathione reductase enzyme on discontinuous SDS-PAGE by silver staining. Separating and stacking gels were prepared 7% and 4% respectively. Glutathione reductase enzyme concentrations in lane 1, 1.2 μg; lane 2, 0.8 μg; lane 3, 0.4 μg.

4.2.2. Determination of Optimum pH by Zero Buffer Extrapolation

To determine the pH optimum of GR, "zero buffer extrapolation" was carried out in order to eliminate the effect of potassium phosphate on enzyme activity. The activity measurements were carried out in phosphate buffers at different pH values (6, 6.5, 7, 7.5, 8, 8.5, 9) and at different concentrations (50 mM, 100 mM, 150 mM, 200 mM). From the activity versus buffer concentration graph the activities at zero buffer concentration were determined by extrapolation (Figure 4.6) and the activity at zero buffer concentration versus pH graph was performed. From the second graph the pH optimum for GR was found to be 7.65 (Figure 4.7) (Landquist, 1955).

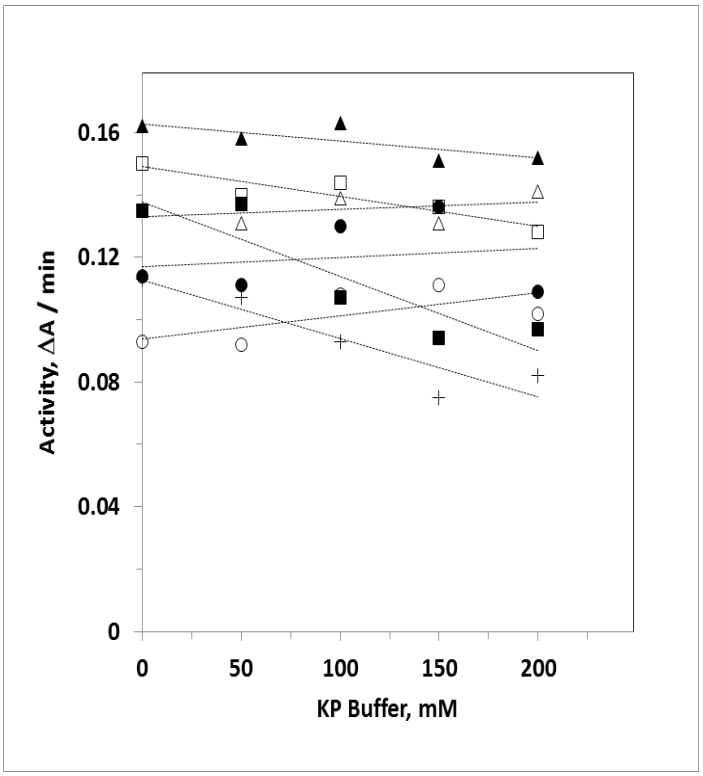

Figure 4.6. Zero buffer extrapolation. ΔA/min vs buffer concentration.

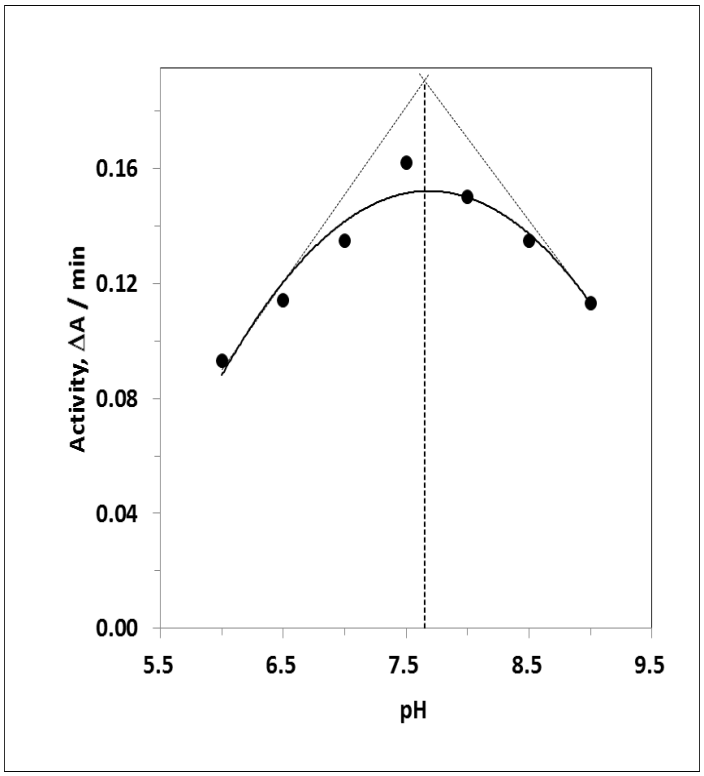

Figure 4.7. ΔA/min vs. pH plot

4.2.3. Determination of Optimum Temperature

The effect of the temperature on the activity of glutathione reductase enzyme was studied by incubating the reaction medium at different temperature points (20°C, 25°C, 30°C, 35°C, 37°C, 40°C, 45°C, 50°C, 55°C, 60°C, 65°C and 70°C). Each measurement was repeated three times and for each temperature point specific activity (U/mg protein) was determined. A graph of specific activity (U/mg protein) versus temperature (°C) was drawn (Figure 4.8.A) and the optimum temperature was found to be 57°C. For the determination of activation energy (E_a), logarithms of specific activities versus reciprocal of temperature in Kelvin was plotted (Figure 4.8.B). On below equations, energy of activation (E_a) and Q_{10} were calculated as 3544 calories and 1.26, respectively,

-Slope = $-E_a/2.3R$

E_a: Activation energy

R: Gas constant

$\mathbf{E_a} = 2.3R\ T_1T_2 \log Q_{10}/10$

Q_{10}: Temperature coefficient

T_1 and **T_2** temperatures in kelvin

4.3. Substrate Kinetics

Kinetic parameters for glutathione reductase enzyme were determined by using different concentrations of GSSG (0.05 mM, 0.1 mM, 0.25 mM, 0.5 mM, 1 mM, 1.5 mM and 2 mM) with respect to the constant NADPH concentration (0.1 mM). V_m and K_m were calculated from interception points on Lineweaver-Burk plot and found to be 220 ± 5 U/mg protein and 100 ± 7 μM, respectively (Figure 4.9. A and B). Also by using different concentrations of NADPH (0.01 mM, 0.015 mM, 0.02 mM, 0.04 mM and 0.1 mM) while keeping GSSG constant (1 mM), kinetic parameters were determined as 209 ± 8 U/mg protein for V_m and 16 ± 2 μM for K_m (Figure 4.10. A and B). All activity measurements were repeated three times and the specific activities (U/mg protein) were used to draw Michaelis-Menten and Lineweaver-Burk plots.

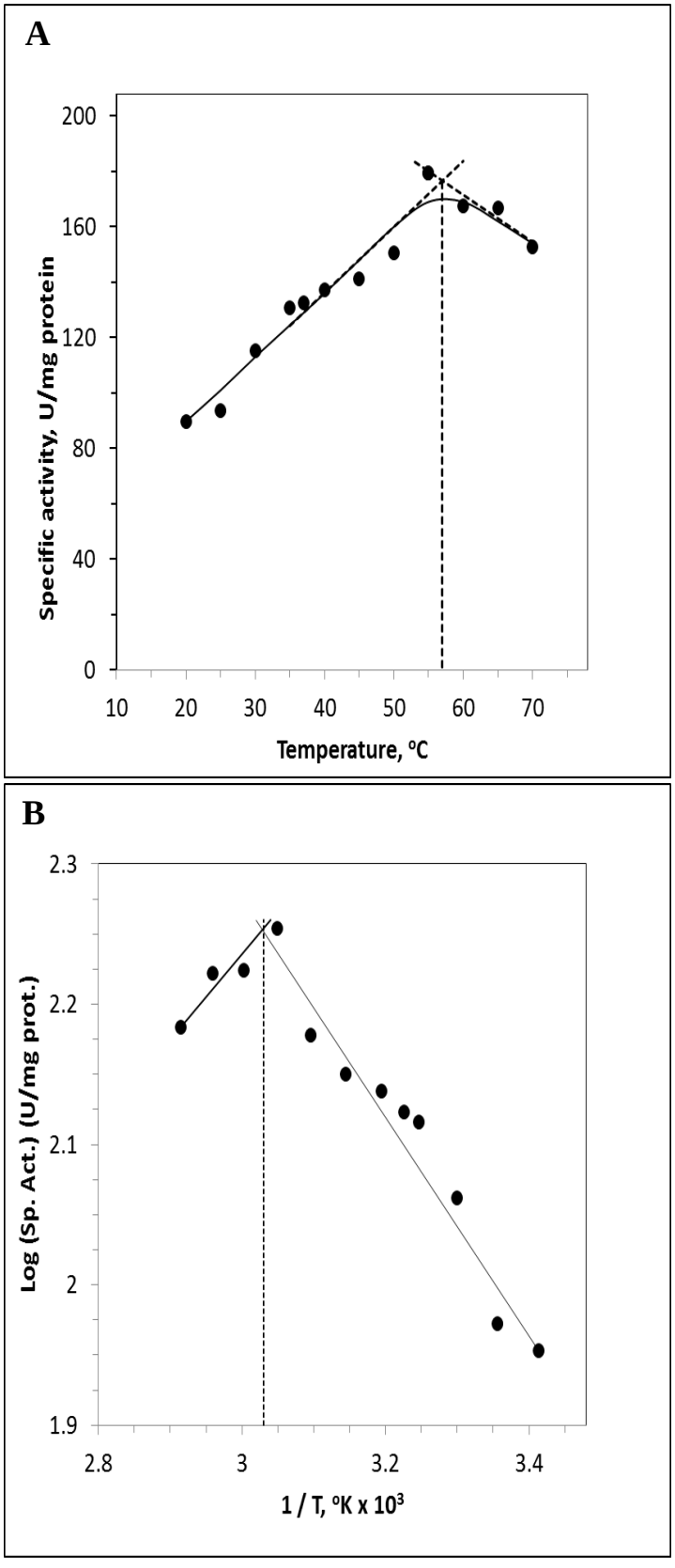

Figure 4.8.A. Specific activity vs. temperature plot. B. Log (Sp. Act.) U/mg protein vs. 1/T plot.

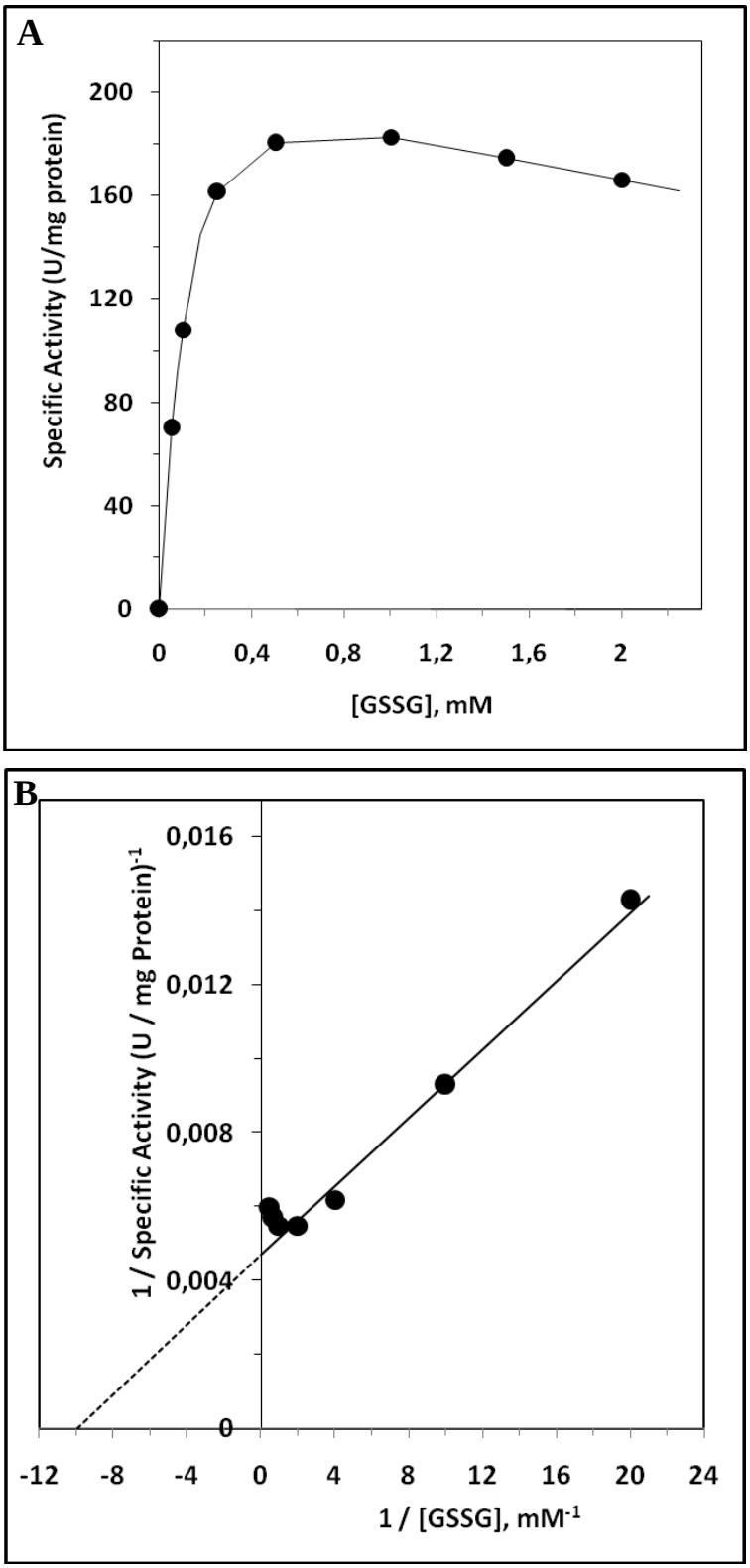

Figure 4.9. Kinetic behavior of glutathione reductase with variable GSSG concentrations (0.05 mM, 0.1 mM, 0.25 mM, 0.5 mM, 1 mM, 1.5 mM and 2 mM). A. Michaelis-Menten plot. B. Lineweaver-Burk plot.

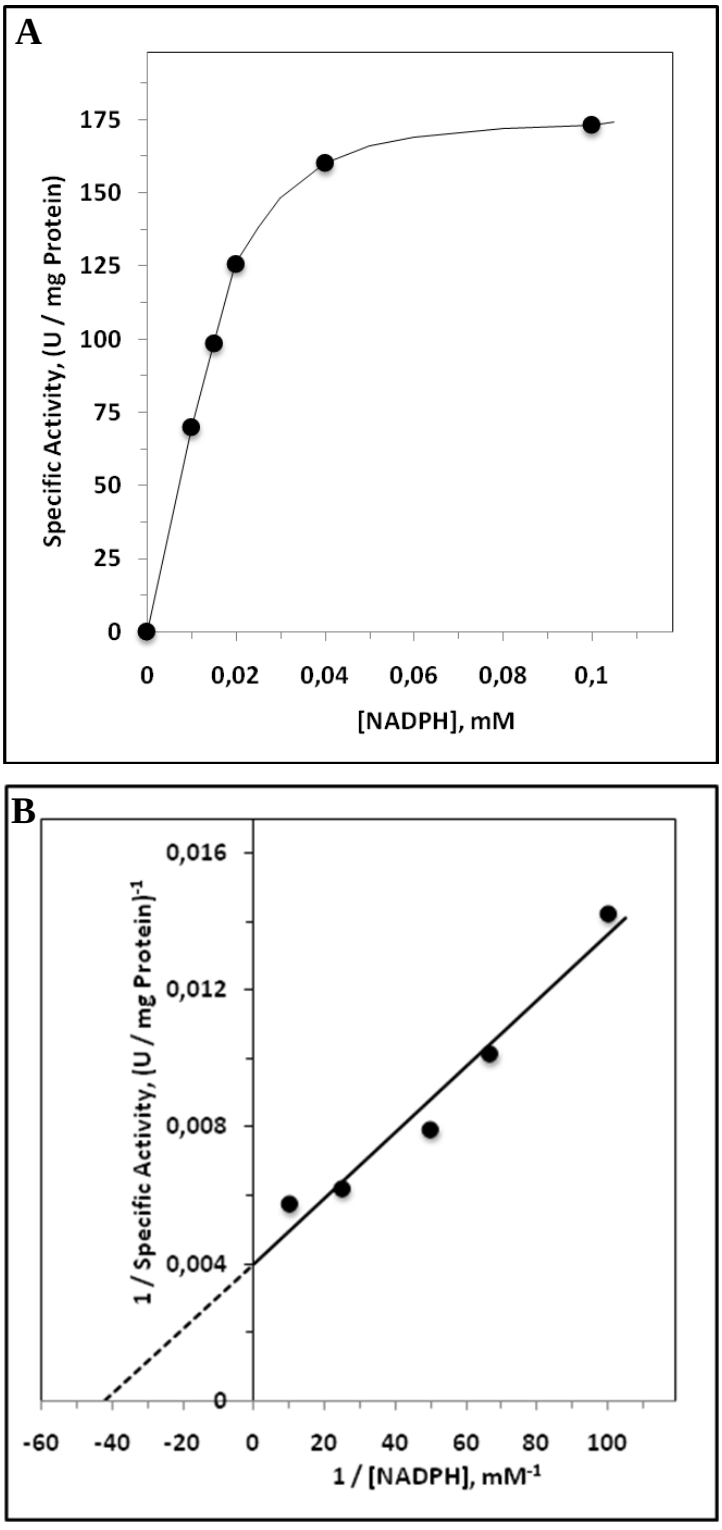

Figure 4.10. Kinetic behavior of glutathione reductase with variable NADPH concentrations (0.01 mM, 0.015 mM, 0.02 mM, 0.04 mM and 0.1 mM). A. Michaelis-Menten plot. B. Lineweaver-Burk plot.

4.4. Inhibitory Kinetic Behaviour of Glutathione Reductase with Hypericin

Glutathione reductase activity was measured by using eight different hypericin concentrations (1 μM, 1.5625 μM, 3.1275 μM, 6.25 μM, 12.5 μM, 25 μM, 50 μM and 100 μM). In the reaction mixture final concentrations of GSSG and NADPH were 1 mM and 0.1 mM, respectively. Each hypericin concentration was studied three times and average specific activities were calculated. As shown in Figure 4.11 hypericin inhibited glutathione reductase enzyme in a dose dependent manner. Although there was a gradual decrease in enzyme activity, inhibition did not reach zero in the concentration range studied. IC_{50} was calculated as 15 μM. In the inhibitory kinetic experiments, four different hypericin concentrations (1 μM, 2 μM, 4 μM and 8 μM) were selected from the area in which linear inhibition was observed.

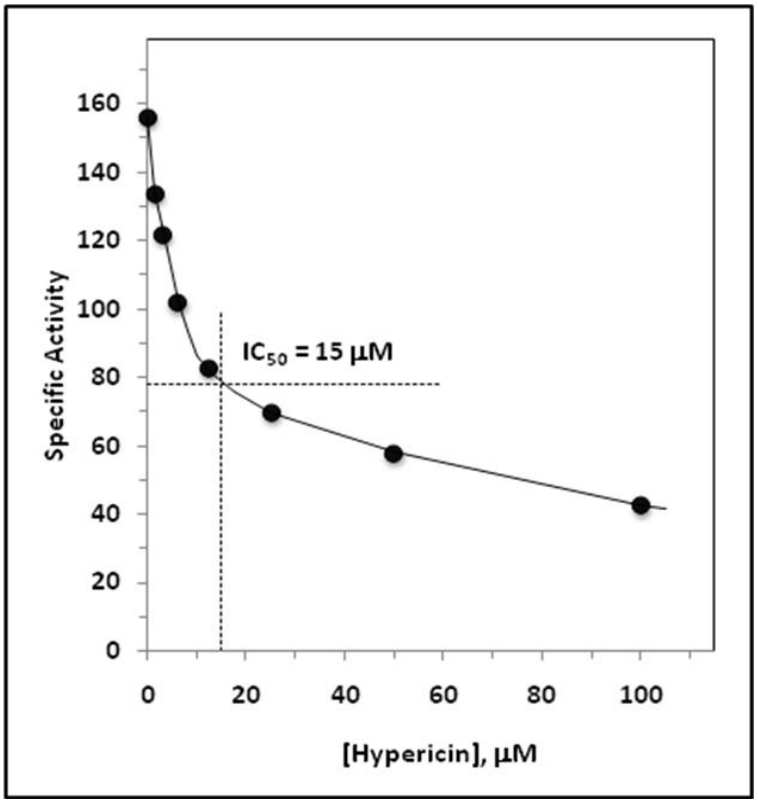

Figure 4.11. Dose dependent inhibition of glutathione reductase by hypericin. [GSSG] = 1 mM, [NADPH] = 0.1 mM, [Hypericin] = 0 μM, 1 μM, 1.5625 μM, 3.1275 μM, 6.25 μM, 12.5 μM, 25 μM, 50 μM and 100 μM.

In inhibitory kinetic experiments with hypericin, first NADPH concentration was kept constant (0.1 mM) and variable GSSG (0.03125 mM, 0.0625 mM, 0.125 mM, 0.25 mM, 0.5 mM and 1 mM) and hypericin (1 μM, 2 μM, 4 μM and 8 μM) concentrations were studied. All activity measurements were performed in triplicates and calculated specific activities were used to draw Michaelis-Menten (Figure 4.12), Lineweaver Burk (Figure 4.13) and Dixon plots (Figure 4.15). When GSSG was the variable substrate, hypericin inhibited glutathione reductase enzyme competitively (Figure 4.13). K_m and K_i were found as 190 ± 40 μM and 2.92 ± 0.73 μM, respectively. V_m was calculated as 242 ± 15 U/mg protein (Figure 4.12 and 4.13).

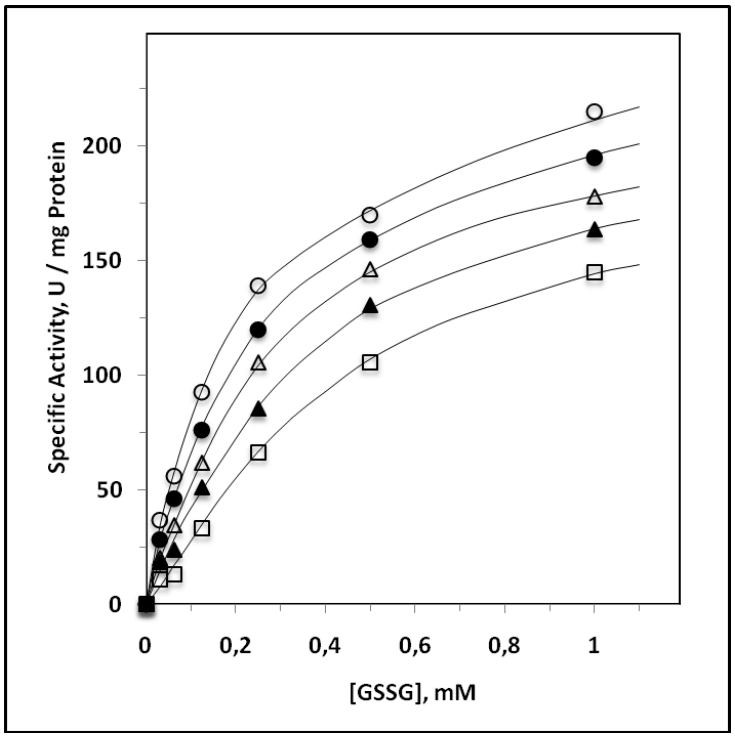

Figure 4.12. Michaelis-Menten plot for glutathione reductase enzyme with different concentrations of hypericin using GSSG as a variable substrate (0.03125 mM, 0.0625 mM, 0.125 mM, 0.25 mM, 0.5 mM and 1 mM). Hypericin concentrations were (○) without hypericin, (●) 1μM, (Δ) 2 μM, (▲) 4 μM, (□) 8 μM.

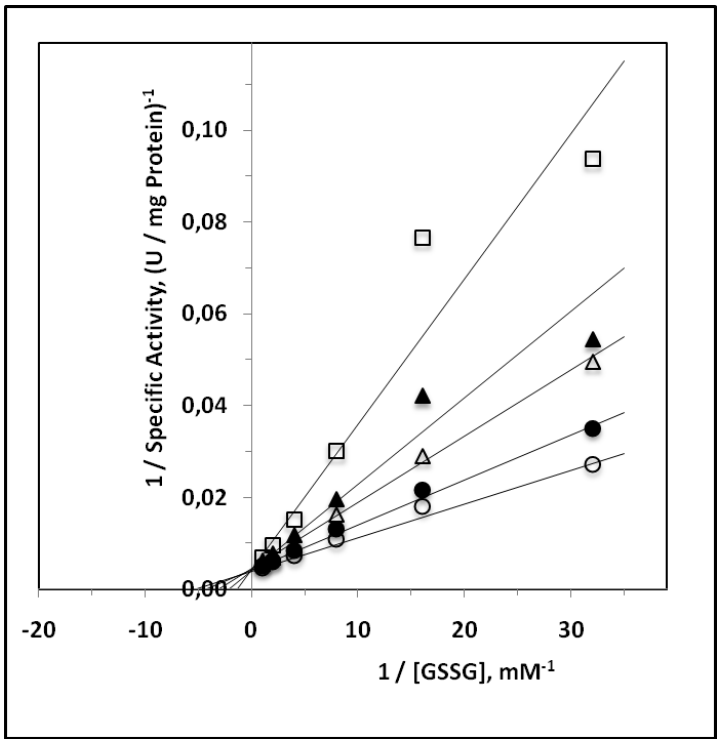

Figure 4.13. Lineweaver-Burk plot for glutathione reductase enzyme with different concentrations of hypericin using GSSG as a variable substrate (0.03125 mM, 0.0625 mM, 0.125 mM, 0.25 mM, 0.5 mM and 1 mM). Hypericin concentrations were (○) without hypericin, (●) 1µM, (Δ) 2 µM, (▲) 4 µM, (□) 8 µM

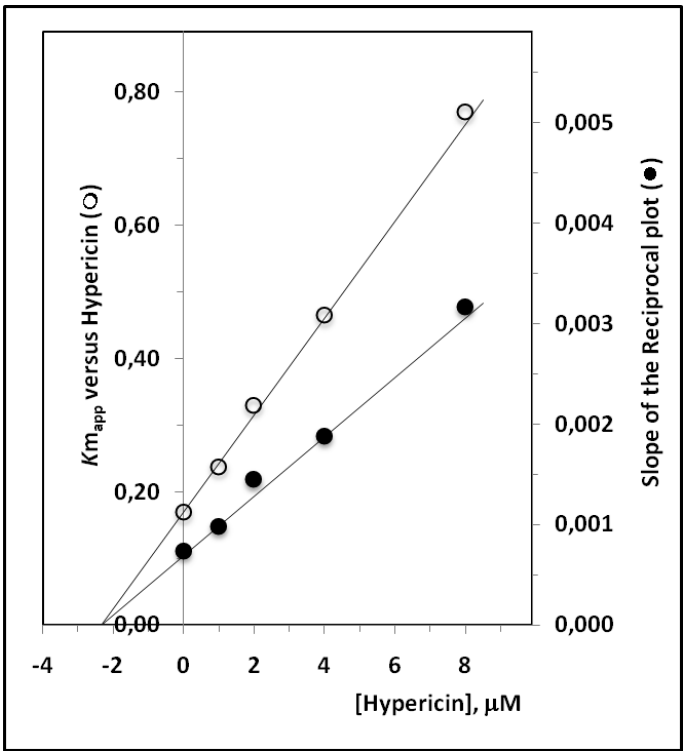

Figure 4.14. K_{mapp} vs. hypericin and slope of the reciprocal vs. hypericin plots

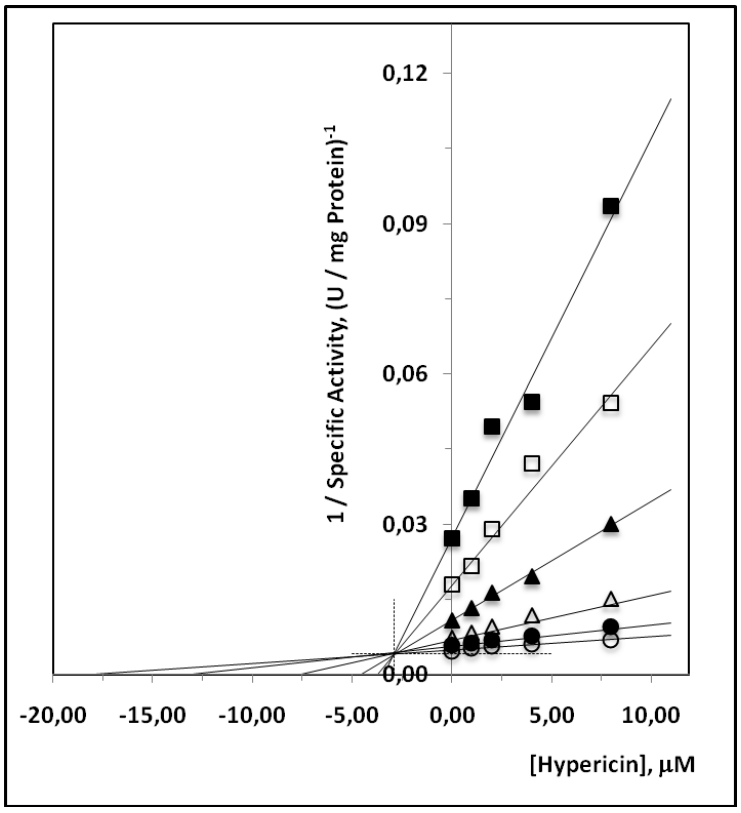

Figure 4.15. Dixon plot for glutathione reductase enzyme. [NADPH]=0.1 mM. [GSSG]: (■) 0.03125; (□), 0.0625; (▲), 0.125; (Δ), 0.25; (●), 0.5; (○), 1 mM. [Hypericin]=0 µM, 1 µM, 2 µM, 4 µM, 8 µM.

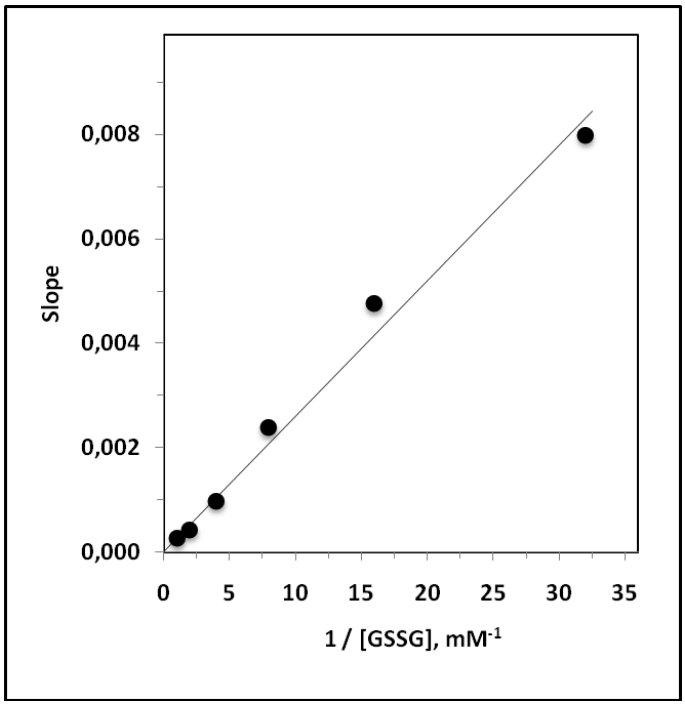

Figure 4.16. Replot of slope of Figure 4.15 versus 1/ [GSSG]

Different NADPH concentrations (0.01 mM, 0.015 mM, 0.02 mM, 0.04 mM and 0.1 mM) were also studied with the same hypericin concentrations (1 μM, 2 μM, 4 μM and 8 μM) while keeping GSSG constant (1 mM). All activity measurements were performed in triplicates and specific activities were used to draw Michaelis-Menten (Figure 4.17), Lineweaver Burk (Figure 4.18) and Dixon plots (Figure 4.20) for the estimation of inhibition type and kinetic parameters. When the variable substrate was NADPH, inhibition type was linear-mixed type competitive and the K_s, K_i and α values were 15.8 ± 1.6 μM, 2.63 ± 0.50 μM and 3.48 ± 1.31, respectively. V_m was calculated as 232 ± 8 U/mg protein.

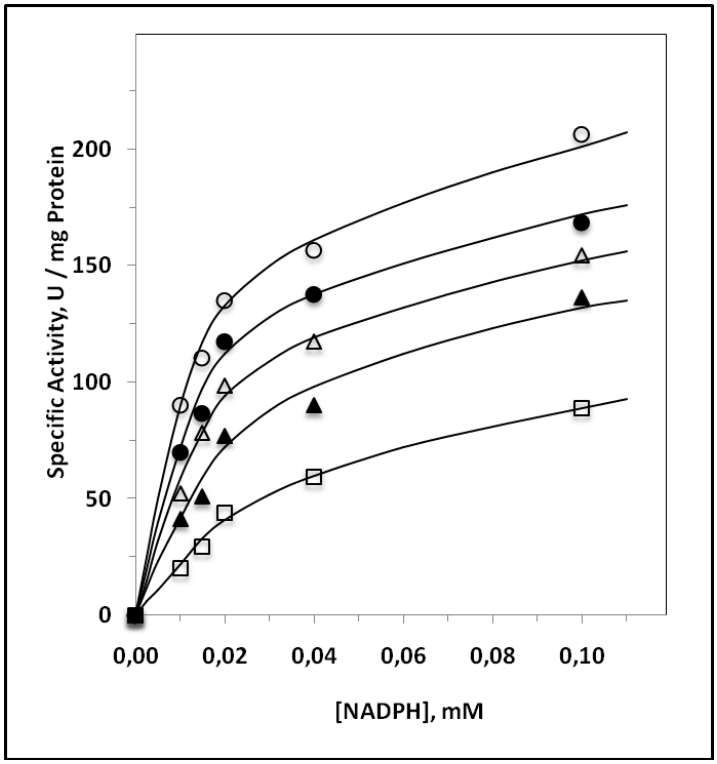

Figure 4.17. Michaelis-Menten plot for glutathione reductase enzyme with different concentrations of hypericin using NADPH as a variable substrate Hypericin inhibition by using NADPH as a variable substrate (0.01 mM, 0.015 mM, 0.02 mM, 0.04 mM and 0.1 mM). [GSSG]=1 mM. Hypericin concentrations were (○) without hypericin, (●) 1µM, (Δ) 2 µM, (▲) 4 µM, (□) 8 µM.

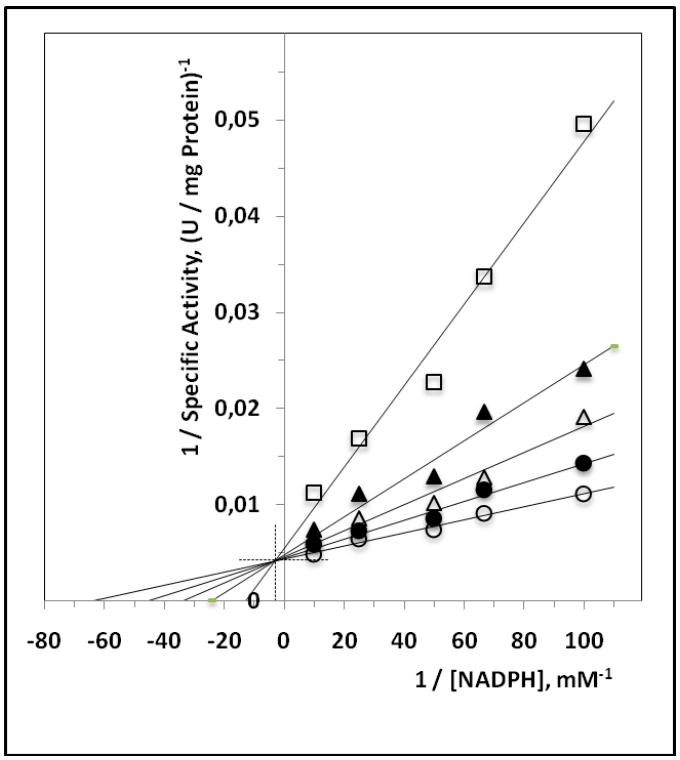

Figure 4.18. Lineweaver-Burk plot for glutathione reductase enzyme with different concentrations of hypericin using NADPH as a variable substrate. NADPH concentrations were 0.01 mM, 0.015 mM, 0.02 mM, 0.04 mM and 0.1 mM and [GSSG]=1 mM. Hypericin concentrations were (○) without hypericin, (●) 1µM, (Δ) 2 µM, (▲) 4 µM, (□) 8 µM.

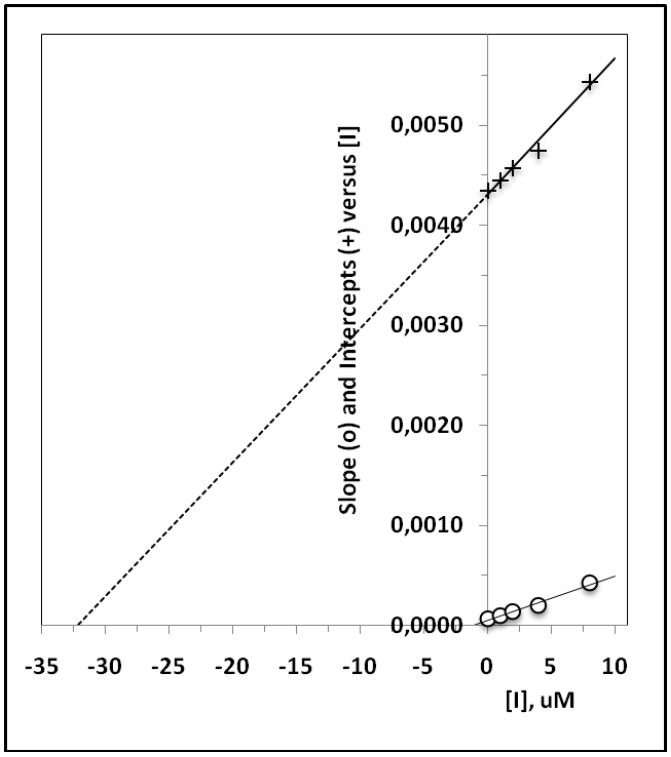

Figure 4.19. Replot of slope and intercept points of Figure 4.18 versus [I]

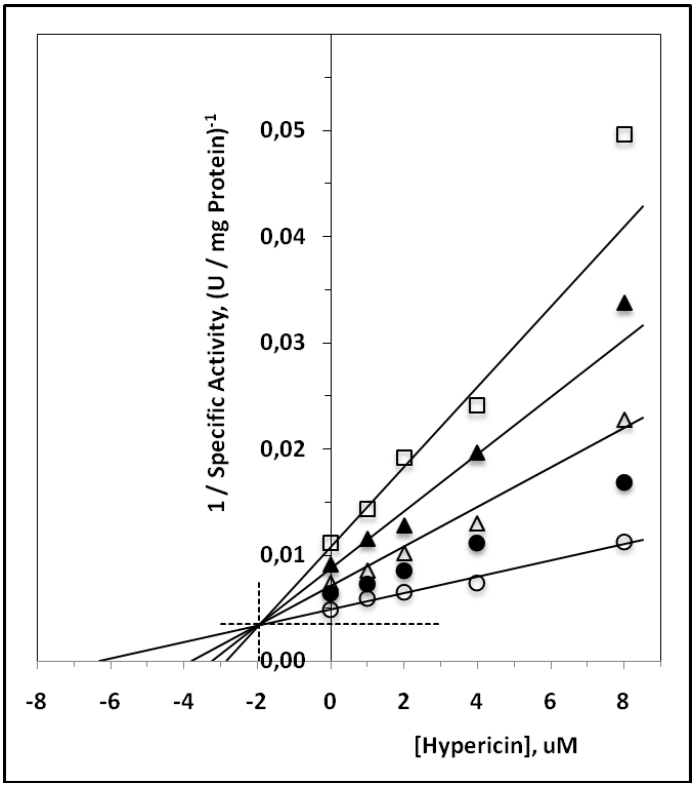

Figure 4.20. Dixon plot for glutathione reductase enzyme. [GSSG]=1 mM. Variable concentration of [NADPH]: (□) 0.01; (▲), 0.015; (Δ), 0.02; (●), 0.04 (○), 0.1 mM. [Hypericin]=0, 1, 2, 4, 8 µM

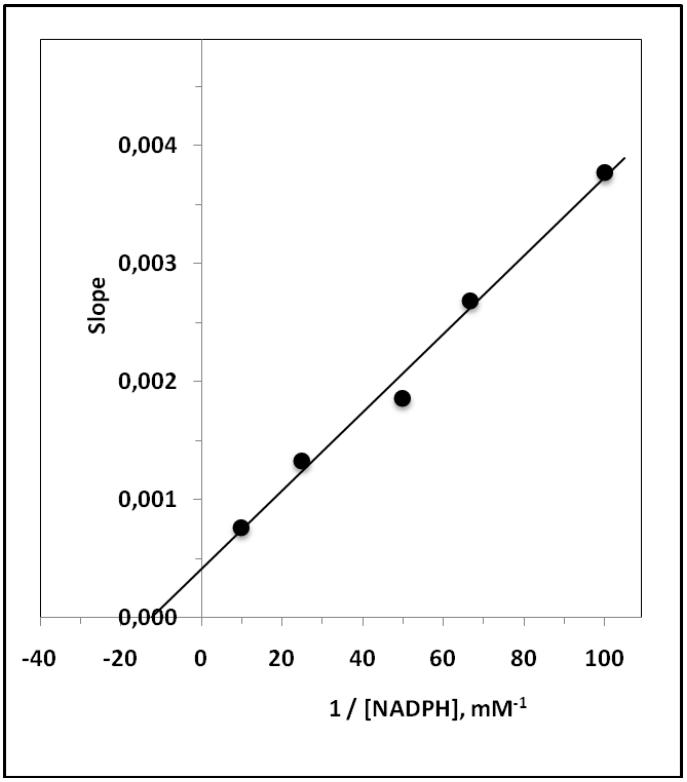

Figure 4.21. Replot of slope of Figure 4.20 versus 1/[NADPH]

5. DISCUSSION

Glutathione reductase (GR) gene in yeast (known as *GLR1*) encodes both mitochondrial and cytosolic forms of the enzyme. Any mutation or deletion will lead to an accumulation of the oxidized glutathione (GSSG) and a loss of reduced glutathione (GSH). *GLR1* gene has two in-frame start codons. The first translation codon (AUG1) creates mitochondrial form and has mitochondrial targeting signal. The second translation codon (AUG17) generates cytosolic form whose translation is more effective that results in abundant cytosolic form. Studies with mutant *GLR1* gene revealed that same mRNA molecule containing these two different start codons is used in the translation of both forms. Based on these findings it was suggested that subcellular distribution of glutathione reductase in mammalian cells might have been conserved as well (Caryn et al., 2013). Amino acid similarity (49.8%) between human and yeast also supported this finding (Collinson and Dawes, 1995). Human GR contains 461 amino acids (Karplus and Schulz, 1987), while yeast form was found to have 467 residues (Collinson and Dawes, 1995). Both forms have an FAD as a prosthetic group and they use NADPH as an electron donor to reduce oxidized glutathione (Untucht-Grau et al., 1981; Takenaka et al., 1988). Distribution of GR in rats has been investigated by using Hilger-Gilford recording spectrophotometer. High GR activity was observed especially in kidney and small intestine. Other tissues and organs like cardiac muscle, skeletal muscle, testis, liver and a number of different glands exhibited low GR activity. Also there was a moderate activity in brain, bladder and adipose tissue (Wendell, 1968).

In this study, GR from baker's yeast was obtained commercially. Before we started our experiments, ammonium sulfate was removed from the enzyme sample by centrifugation. Pellet was used in all following experiments. The purity and the subunit molecular weight of the enzyme were determined by native-polyacrylamide gel electrophoresis (native-PAGE) and SDS-polyacrylamide gel electrophoresis (SDS-PAGE). Coomassie Brilliant Blue R-250, silver and activity stainings were carried out to visualize protein bands on native-PAGE. In native–PAGE, single protein band was observed (Figures 4.2 and 4.3). In SDS-PAGE, protein markers are used for the estimation of subunit molecular weight of GR. Coomassie Brilliant Blue R-250 and silver stainings also revealed a single protein band and by comparing the

migration distance of GR and the protein markers, subunit molecular weight was calculated as 49 kDa (Figures 4.4 and 4.5) which is consistent with the literature. Previously, researchers found the subunit molecular weight of yeast GR as 51 kDa (Hou et al., 2004). Can et al. calculated the subunit Mr of rat kidney GR as 53 kDa (Can B et al., 2010), and for human and bovine erythrocytes subunit molecular weight of GR was found as 58 kDa (Ogüs and Ozer, 1998; Erat et al., 2003). Mavis and Stellwagen first calculated the subunit molecular weight of yeast GR as 64 kDa, but in the presence of 5 M guanidine hydrochloride they observed that the molecular weight of the enzyme was reduced to 51.5 kDa (Mavis and Stellwagen, 1968). This must be due to the breakdown of more hydrogen bonds and more SDS molecules are bound to the enzyme resulting in the increase of charge mass ratio.

In order to determine the pH optimum and to eliminate the buffer effect, "zero buffer extrapolation method" was applied. The activity measurements were carried out in phosphate buffers at different pH values (6, 6.5, 7, 7.5, 8, 8.5, 9) and at different concentrations (50 mM, 100 mM, 150 mM, 200 mM). From the activity versus buffer concentration graph the activities at zero buffer were determined by extrapolation (Figure 4.6) and the activity at zero buffer concentration versus pH graph was performed. From the second graph the pH optimum for GR was found to be as 7.65 (Figure 4.7) (Landqvist, 1955). This result is close to pH optimum of human erythrocyte GR (pH 7.20) and bovine erythrocyte GR (pH 7.3) but higher than the pH optimum reported for rat kidney GR (pH 6.5) (Ogüs and Ozer, 1998; Erat al., 2003: Can et al., 2010). This discrepancy could be explained by the differences in the functions of the tissues.

To evaluate the optimum temperature of the enzyme, the activity of the enzyme was measured at different temperatures (20°C, 25°C, 30°C, 35°C, 40°C, 45°C, 50°C, 55°C, 60°C, 65°C and 70°C). The temperature optimum, activation energy (E_a) and Q_{10} were calculated as 57^{o}C, 3,544 calories and 1.26, respectively (Figure 4.8.A and B). In comparison with the previously published data our findings are consistent with the report of Erat et al. in which optimum temperature of bovine erythrocyte GR was found to be 55°C (Erat et al., 2003). GR purified from rat kidney had an optimum temperature of 65°C, the activation energy (E_a) and the temperature

coefficient (Q_{10}) were found to be 7.02 kcal/mol and 1.42, respectively (Can et al., 2010). These results shows GR has stability and tolerance to high temperature points.

The values of kinetic parameters in the absence of inhibitor were determined as K_{mGSSG} 100 ± 7 μM, K_{mNADPH} 16 ± 2 μM. In the other kinetic studies with yeast GR K_{mGSSG} and K_{mNADPH} were calculated as 90±12 μM and 30±4 μM, respectively (Tandoğan and Ulusu, 2007). Same kinetic parameter (K_m) for yeast GR at variable GSSG and NADPH were also determined as 55 μM and 3.8 μM, respectively (Massey and Williams, 1965). GR purified from rat liver revealed K_{mGSSG} as 56.7 ± 0.4 μM and K_{mNADPH} as 7.9 ± 0.6 μM (Carlberg and Mannervik, 1975). K_{mGSSG} and K_{mNADPH} were determined for GR from *E coli* as 97 ± 12 μM and 22 ± 2 μM, respectively (Bashir et al., 1995).

Hypericin inhibition was tested by using different hypericin concentrations ranging between 1-100 μM while keeping the concentration of NADPH (0.1 mM) and GSSG (1 mM) constant. The activity of the enzyme was gradually decreasing as hypericin concentration increased meaning that hypericin has an inhibitory effect on GR with quite low half maximal inhibitory concentration (IC_{50}) which was calculated as 15 μM (Figure 4.11). Considering the half-lives of hypericin and pseudohypericin which were found as 24.8 to 26.5 hours and 16.3 to 36.0 hours, respectively (Staffeldt et al., 1994), low IC_{50} indicated hypericin could have long term inhibitory effect on GR.

The enzyme was further tested in inhibitory kinetic experiments in which 1, 2, 4, 8 μM hypericin concentrations were chosen to be used. Competitive type of inhibition was observed when the GSSG was the variable substrate with K_m, K_i and V_m values of 190 ± 40 μM, 2.92 ± 0.73 μM and 242 ± 15 U/mg protein, respectively (Figure 4.12 and 4.13). Inhibition type was linear-mixed type competitive with variable NADPH concentrations and the K_s, K_i, α and V_m values were 15.8 ± 1.6 μM, 2.63 ± 0.50 μM, 3.48 ± 1.31 and 232 ± 8 U/mg protein, respectively (Figure 4.17 and 4.18). The competitive inhibition shows that hypericin binds to the substrate binding site and prevents the binding of GSSG. Therefore it increases appearent K_m. Since the binding sites of NADPH and GSSG are close to each other, linear-mixed type

competitive inhibition was observed with variable NADPH, which means hypericin affects binding of NADPH, too.

GR is considered as one of the major components of antioxidant enzyme system for cellular defense against oxidative stress (Willmore and Storey, 2007). It is a promising target for the improvement of antimalarial agents which could be used to decrease anti-malarial resistance (Seefeldt et al., 2005). Malaria parasite has its own glutathione (GSH) redox in which any alteration in the GSH level is associated with the resistance to antimalarial drugs. Several enzymes in this redox system have been investigated as a target for anti-malarial drugs including GR. Inhibition of the GR by methylene blue (MB) and eosin B leads to death of the parasite (Pastrana-Mena et al., 2010). GR has a critical role in the thiol redox state (TRS) hemostasis by maintaining a high GSH/GSSG ratio. It could be an important parameter for increasing the level of TRS because inhibition of the enzyme leads to a decrease in GSH/GSSG ratio (Asmis et al., 2005).

In the literature, anti-depressant drugs have been elucidated to act as an inhibitor on the antioxidant enzymes such as inhibition of human placental glutathione S-transferase-π by fluoxetine (Dalmizrak et al., 2016), amitriptyline and clomipramine (tricyclic antidepressants) (Dalmizrak et al., 2011) and sertraline (Dalmizrak et al., 2012). Amitriptyline by inhibiting both glutathione S-transferase pi and alpha may have role in cancer treatment (Kulaksiz-Erkmen et al., 2013).

Hypericin has an inhibitory effect on other antioxidant enzymes such as glutathione S-transferase pi (GST-pi). GST-pi purified from human placenta was inhibited competitively by hypericin when reduced glutathione and 1-chloro-2,4-dinitrobenzene (CDNB) were used as variable substrates (Dalmizrak et al., 2012). On other hand noncompetitive type of inhibition was demonstrated when erythrocyte GST-pi enzyme was inhibited by hypericin (Turk et al., 2015). Tuna et al. studied the effect of hypericin on rat small intestine GST isoenzymes, alpha and pi and demonstrated that when the variable substrate was GSH, inhibition type was uncompetitive for GST-alpha and noncompetitive for GST-pi. Noncompetitive and competitive inhibitions were observed for GST-alpha and GST-pi, respectively, when the variable substrate was CDNB (Tuna, G et al., 2010).

In the presence of visible light and oxygen molecule, hypericin has a powerful photosensitizer action which can be used in photodynamic therapy to kill cancer cells by generating singlet oxygen and superoxide anion (Thomas et al., 1992; Diwu and Lown, 1993) which leads to apoptosis (Ali and Olivo, 2002; Mikeš et al., 2007), autophagy (Buytaert et al., 2006; Rubio et al., 2012) and necrosis (Du et al., 2003; Mikeš et al., 2007). The uptake mechanism of hypericin into cellular system is not well known yet but there is a promising study shows hypericin might enter the cells through passive transcellular diffusion (temperature-dependent diffusion) (Sattler et al., 1997) or by partitioning, pinocytosis and endocytosis (Siboni et al., 2002). Co-labeling with hypericin and fluorescent dyes which are specific for organelles demonstrated that hypericin fuses and accumulates in the cell membranes of the endoplasmic reticulum, the Golgi apparatus, lysosomes and mitochondria (Ali and Olivo, 2002; Galanou et al., 2008; Mikeš et al., 2011). However hypericin might be affected during cellular uptake and subcellular localization depending on its lipophilicity, incubation concentrations and/or interaction with serum lipoproteins (Crnolatac et al., 2005; Galanou et al., 2008; Kascakova et al., 2008).

Researchers proposed that hypericin have an antidepressant activity for those who suffer from depression (Kenneth et al., 2011). Studies on the rat brain mitochondria shows that hypericin has great inhibitory potential on monoamine oxidase (MAO-A and –B) enzymes (Suzuki et al., 1984; Awang, 2009). MAO is responsible for the inhibition of amine neurotransmitter degradation which increases their levels in synaptic cleft. Hypericin has a strong affinity for sigma receptors, which regulate dopamine levels. It also acts as a receptor antagonist at adenosine, benzodiazepine, GABA-A, GABA-B and inositol triphosphate receptors which regulate action potentials caused by neurotransmitters (Chavez and Chavez 1997; Jellin et al., 2002). Further study showed that long-term administration of St. John's wort and its active constituent hypericin modifies the levels of neurotransmitters in brain regions (Butterweck et al., 2002).

Hypericin has been shown to inhibit the growth of viruses by preventing budding and shedding or it has influence on the cell membranes of murine Friend leukemia virus *in vitro* (Meruelo Da et al., 1988), equine infectious anemia virus (EIAV) (Kraus et al., 1990), influenza virus (Tang et al., 1990), duck hepatitis B

virus (Moraleda et al., 1993), murine immunodeficiency virus (Lavie et al., 1989). Vesicular stomatitis viruses were photodynamically inactivated by hypericin (Lenard et al., 1993). In the presence of light hypericin completely inhibits bovine diarrhea virus (BVDV) *in vitro* (Jeffrey et al., 2001).

It was found that GR is inhibited by micromolar concentrations of hypericin. As a result, in addition of producing ROS to kill cancer cells in PDT, inhibition of GR will also contribute to the sensitization of cancer cells and thus will potentiate the therapeutic effect of hypericin but these results still need conformation by *in vivo* studies (animal studies).

6. CONCLUSION

In this study, characterization and inhibitory effect of hypericin on glutathione reductase (GR) was explored. The purity of enzyme was confirmed by native and SDS-PAGE. The enzyme was further used for characterization in terms of its optimum pH and optimum temperature. Kinetic experiments were performed by using different concentrations of GSSG and NADPH to calculate V_m and K_m values of the enzyme. Finally, possible inhibitory behavior of hypericin on GR was tested by using different inhibitor concentrations and inhibitory kinetic parameters were calculated for variable GSSG and NADPH concentrations.

In both native and SDS-PAGE single protein band was observed confirming the purity of the enzyme sample. SDS-PAGE was also used to appraise the subunit molecular weight of the enzyme and it was calculated as 49 kDa. Optimum pH and optimum temperature of GR were found to be 7.65 and 57^{o}C, respectively. Energy of activation (E_a) and temperature coeffiecient (Q_{10}) were found to be 3,544 calories and 1.26, respectively. Hypericin was found to inhibit GR in a dose dependent manner with an IC_{50} value of 15 μM. Inhibitory kinetic studies revealed competitive and linear-mixed type competitive inhibitions when GSSG and NADPH were used as variable substrates, respectively. When the variable substrate was GSSG, K_m and K_i were found as 190 ± 40 μM and 2.92 ± 0.73 μM, respectively. On the other hand, when the variable substrate was NADPH, K_s, K_i and α values were 15.8 ± 1.6 μM, 2.63 ± 0.50 μM and 3.48 ± 1.31, respectively.

Further *in vivo* studies should be performed on glutathione reductase and its inhibition mechanism by hypericin in order to understand the role of GR on the level of GSH/GSSG and to evaluate its anticancer or antimalarial properties.

REFERENCES

Adams, L., Franco, M.C., Estevez, A.G. (2015). Reactive nitrogen species in cellular signaling. *Exp Biol Med (Maywood).* 240(6):711-7.

Agar, N.S., Sadrzadeh, S.M., Hallaway, P.E., Eaton, J.W. (1986). Catalase. A somatic oxidant defense. *J Clin Invest*. 77(1):319–321.

Agostinis, P., Vantieghem A., Merlevede, W., de Witte, P.A.M. (2002). Hypericin in cancer treatment: More light on the way. *Int J Biochem Cell Biol*. 34:221–41.

Ali, S.M., Olivo, M. (2002). Bio-distribution and subcellular localization of Hypericin and its role in PDT induced apoptosis in cancer cells. *Int J Oncol*. 21, 531–540.

Allen, C.L., Bayraktutan, U. (2009). Oxidative stress and its role in the pathogenesis of ischaemic stroke. *Int J Stroke*. 4(6):461-70.

Arthur, J.R. (2000). The glutathione peroxidases. *Cell Mol Life Sci*. 57.1825–1835.

Asmat, U., Abad, K. and Ismail, K. (2016). Diabetes mellitus and oxidative stress-A concise review. *Saudi Pharm J*. 24(5):547–553.

Asmis, R., Wang, Y., Xu, L., Kisgati, M., Begley, J.G. and Mieyal, J.J. (2005). A novel thiol oxidation-based mechanism for adriamycin-induced cell injury in human macrophages. *FASEB J*. 19:1866–1868.

Assad, A., Mohammad, Reza, Z., Abolghasem, J. and Morteza, S. (2011). Comparing of the effects of hypericin and synthetic antidepressants on the expression of morphine-induced conditioned place preference. *Iran J Pharm Res*. 10(3):619–626.

Auten, R.L. and, Davis J.M. (2009). The nature of the injury will ultimately depend on specific molecular interactions, cellular locations, and timing of the insult (2009). *Pediatric Research.* 66(2):121-7.

Awang D.V.C. (2009). *Tyler's Herbs of Choice: The Therapeutic Use of Phytomedicinals.* Boca Raton, Florida: CRC Press, Taylor and Francis Group.

Baker, R.D., Baker, S.S., LaRosa, K., Whitney, C., Newburger, P.E. (1993). Selenium regulation of glutathione peroxidase in human hepatoma cell line Hep3B. *Arch Biochem Biophys.* 304(1):53-7.

Barathan, M., Mariappan, V., Shankar, E.M., Abdullah, B.J., Goh, K.L., Vadivelu, J. (2013). Hypericin-photodynamic therapy leads to interleukin-6 secretion by HepG2 cells and their apoptosis via recruitment of BH3 interacting domain death agonist and caspases. *Cell Death Dis*. 27;4:e697.

Bashir, A., Perham, R.N., Scrutton, N., Berry, A. (1995). Altering kinetic mechanism and enzyme stability by mutagenesis of the dimer interface of glutathione reductase. *Biochem J*. 312:527–533.

Bauer, H., Fritz-Wolf, K., Winzer, A., Kühner, S., Little, S., Yardley, V., Vezin, H., Palfey, B., Schirmer, R.H., Davioud-Charvet, E. (2006). A fluoro analogue of the menadione derivative 6-[2'-(3'-methyl)-1', 4'-naphthoquinolyl] hexanoic acid is a suicide substrate of glutathione reductase. Crystal structure of the alkylated human enzyme. *J Am Chem Soc*. 128(33):10784-94.

Becker, K., Pons-Kühnemann, J., Fechner, A., Funk, M., Gromer, S., Gross, H.J., Grünert, A., Schirmer, R.H. (2005). Effects of antioxidants on glutathione levels and clinical recovery from the malnutrition syndrome kwashiorkor-a pilot study. *Redox Rep*. 10(4):215-26.

Berkholz, D.S., Faber, H.R., Savvides, S.N., Karplus, P.A. (2008). Catalytic cycle of human glutathione reductase near 1 Å resolution. *J Mol Biol*. 382(2):371–384.

Betteridge, D.J. (2000). What is oxidative stress. *Metabolism.* 49(2 Suppl 1):3-8.

Blum, H., Beier, H. and Gross, H.J. (1987). Improved silver staining of plant protein, RNA and DNA in polyacrylamide gels. *Electrophoresis*. 8(2):93-99.

Bocchino, M., Agnese, S., Fagone, E., Svegliati, S., Grieco, D., Vancheri, C., Gabrielli, A., Sanduzzi, A., Avvedimento, E.V. (2010). Reactive oxygen species are required for maintenance and differentiation of primary lung fibroblasts in idiopathic pulmonary fibrosis. *PLoS One*. 16;5(11):e14003.

Bonomini, F., Tengattini, S., Fabiano, A., Bianchi, R., Rezzani, R. (2008). Atherosclerosis and oxidative stress. *Histol Histopathol.* 23(3):381-90.

Borrás, C., Esteve, J.M., Viña, J. R., Sastre, J., Viña, J., Pallardó, F.V. (2004). Glutathione regulates telomerase activity in 3T3 fibroblasts. *J Biol Chem.* 279(33):34332-5.

Bradford, M.M. (1976). A rapid and sensitive method for the quantitation of microgram quantities of protein utilizing the principle of protein-dye binding. *Anal Biochem*. 72:248-54.

Bryan, N.S., Bian, K., Murad, F. (2009). Discovery of the nitric oxide signaling pathway and targets for drug development. *Front Biosci (Landmark Ed).* 14:1-18.

Butterweck, V., Böckers, T., Korte, B., Wittkowski W., Winterhoff, H. (2002). Long-term effects of St. John's wort and hypericin on monoamine levels in rat hypothalamus and hippocampus. *Brain Res*. 930(1-2):21-9.

Buytaert, E., Callewaert, G., Hendrickx, N., Scorrano, L., Hartmann, D., Missiaen, L. (2006). Role of endoplasmic reticulum depletion and multidomain proapoptotic BAX and BAK proteins in shaping cell death after hypericin-mediated photodynamic therapy. *FASEB J*. 20:756–758.

Cadenas, E., Davies, K.J. (2000). Mitochondrial free radical generation, oxidative stress, and aging. *Free Radic Biol Med*. 29(3-4):222-30.

Can, B., Kulaksiz Erkmen, G., Dalmizrak, O., Ogus, I., Ozer, N. (2010). Purification and characterization of rat kidney glutathione reductase. *Protein J*. 29(4):250-6.

Carlberg, I., Mannervik, B. (1975). Purification and characterization of the flavoenzyme glutathione reductase from rat liver. *J Biol Chem.* 250(14):5475–5480.

CC treatment. (2015). Free Radicals in the Body–Oxidative Stress and the Antioxidant Response. http://cancercelltreatment.com/2015/08/13/free-radicals-in-the-body-oxidative-stress-and-the-antioxidant-response/. 20/11/2016.

Cereser, C., Boget, S., Parvaz, P., Revol, A.Y. (2001). Thiram-induced cytotoxicity is accompanied by a rapid and drastic oxidation of reduced glutathione with consecutive lipid peroxidation and cell death. *Toxicology*. 163(2-3):153-62.

Chavez, M.L., Chavez, P.I. (1997). Saint John's Wort. *Hosp Pharm.* 32(12):1621–32.

Chiricolo, M., Tazzari, P.L., Abbondanza, A., Dinota, A., Battelli M.G. (1991). Cytotoxicity of, and DNA damage by, active oxygen species produced by xanthine oxidase. *FEBS Letters*. 1291(2):173–176.

Collinson, L.P., Dawes, I.W. (1995). Isolation, characterization, and overexpression of the yeast gene, GLR1, encoding glutathione reductase. *Gene*. 156(1):123-7.

Crnolatac, I., Huygens A., van Aerschot A., Busson R., Rozenski J., de Witte P.A. (2005). Synthesis, in vitro cellular uptake and photo-induced antiproliferative effects of lipophilic hypericin acid derivatives. *Bioorg Med Chem.* 13:6347–6353.

Dalmizrak, O., Kulaksiz-Erkmen G., Ozer, N. (2016). Fluoxetine-induced toxicity results in human placental glutathione S-transferase-π (GST-π) dysfunction. *Drug Chem Toxicol.* 39(4):439-44.

Dalmizrak, O., Kulaksiz-Erkmen, G., Ozer, N. (2011). The inhibition characteristics of human placental glutathione S-transferase-π by tricyclic antidepressants: amitriptyline and clomipramine. *Mol Cell Biochem*. 355(1-2):223-31.

Dalmizrak, O., Kulaksiz-Erkmen, G., Ozer, N. (2012). Evaluation of the in vitro inhibitory impact of hypericin on placental glutathione S-transferase pi. *Protein J.* 31(7):544-9.

Dalmizrak, O., Kulaksiz-Erkmen, G., Ozer, N. (2012). Possible prenatal impact of sertraline on human placental glutathione S-transferase-π. *Hum Exp Toxicol*. 31(5):457-64.

Dhalla, N.S., Temsah, R.M., Netticadan, T. (2000). Role of oxidative stress in cardiovascular diseases. *J Hypertens.* 18(6):655-73.

Di Filippo, C., Cuzzocrea, S., Rossi, F., Marfella, R., D'Amico, M. (2006). Oxidative stress as the leading cause of acute myocardial infarction in diabetics. *Cardiovasc Drug Rev.* 24(2):77-87.

Diwu, Z., Lown, J.W. (1993). Photosensitization with anticancer agents. 17. EPR studies of photodynamic action of hypericin: formation of semiquinone radical and activated oxygen species on illumination. *Free Radic Biol Med.* 14:209–215.

Dostalek, M., Hardy, K.D., Milne, G.L., Morrow, J.D., Chen, C., Gonzalez, F J., Gu, J., Ding X, Johnson D.A, Johnson J.A, Martin M.V, Guengerich F.P. (2008). Development of oxidative stress by cytochrome P450 induction in rodents is selective for barbiturates and related to loss of pyridine nucleotide-dependent protective systems. *J Biol Chem*. 283(25):17147-57.

Droge, W. (2002). Free radicals in the physiological control of cell function. *Physiol Rev.* 82:47–95.

Du, H.Y., Olivo, M., Tan B.K., Bay, B.H. (2003). Hypericin-mediated photodynamic therapy induces lipid peroxidation and necrosis in nasopharyngeal cancer. *Int J Oncol*. 23:1401–1405.

Erat, M., Sakiroglu, H., Ciftci, M. (2003). Purification and characterization of glutathione reductase from bovine erythrocytes. *Prep Biochem Biotechnol*. 33(4):283-300.

Finkel, T., Nikki, J. Holbrook. (2000). Oxidants, oxidative stress and the biology of ageing. *Nature*. 408:239-247.

Fukai, T., Ushio-Fukai, M. (2011). Superoxide dismutases: Role in redox signaling, vascular function, and diseases. *Antioxid Redox Signal*. 15(6):1583–1606.

Galanou, M.C., Theodossiou, T.A., Tsiourvas, D., Sideratou, Z., Paleos, C.M. (2008). Interactive transport, subcellular relocation and enhanced phototoxicity of

hypericin encapsulated in guanidinylated liposomes via molecular recognition. *Photochem. Photobiol*. 84:1073–1083.

Garg, A.D., Bose, M., Ahmed, M.I, Bonass, W.A., Wood, S.R. (2012). In vitro studies on erythrosine-based photodynamic therapy of malignant and pre-malignant oral epithelial cells. *PLoS One*. 7(4):e34475.

Gizi, A., Papassotiriou, I., Apostolakou, F., Lazaropoulou, C., Papastamataki, M., Kanavaki, I., Kalotychou, V., Goussetis, E., Kattamis, A., Rombos, I., Kanavakis, E. (2011). Assessment of oxidative stress in patients with sickle cell disease: The glutathione system and the oxidant-antioxidant status. *Blood Cells Mol Dis*. 46(3):220-5.

Gonzalez, F.J. (2005). Role of cytochromes P450 in chemical toxicity and oxidative stress: studies with CYP2E1. *Mutat Res*. 569(1-2):101-10.

Graubaum, W.B. (1981). *Handbook for Forensic Individualization of Human Blood and Blood Stains.* Berkeley, CA: Sartorius.

Hames, B.D. (1998). *Gel Electrophoresis of Protein*. New York: Oxford University Press.

Head C.S., Luu, Q., Sercarz, J., Saxton, R. (2006). Photodynamic therapy and tumor imaging of hypericin-treated squamous cell carcinoma. *World J Surg Oncol*. 4:87.

Henricks, P.A., Nijkamp, F.P. (2001). Reactive oxygen species as mediators in asthma. *Pulm Pharmacol Ther*. 14(6):409-20.

Herzenberg, A.L., De Rosa, C.S., Dubs, J.G., Roederer, M., Anderson,T.M., Ela, W.S. and Deresinski, C.S. (1997). Glutathione deficiency is associated with impaired survival in HIV disease. *Proc Natl Acad Sci U S A*. 4;94(5):1967–1972.

Hou, W.C., Liang, H.J., Wang, C.C., Liu, D.Z. (2004). Detection of glutathione reductase after electrophoresis on native or sodium dodecyl sulfate-polyacrylamide gels. *Electrophoresis*. 25(17):2926-31.

Iskusnykh, I.Y., Popova, T.N., Agarkov, A.A, Pinheiro de Carvalho, M.Â., Rjevskiy, S.G. (2013). Expression of glutathione peroxidase and glutathione reductase and level of free radical processes under toxic hepatitis in rats. *Journal of Toxicology*. 13:1-9.

Jacobson, J.M., Feinman, L., Liebes, L., Ostrow, N., Koslowski, V., Tobia. A., Bernard, E., Lee, C.D., Spritzler J. and Prince A.M. (2001). Pharmacokinetics, safety, and antiviral effects of hypericin, a derivative of St. John's wort plant, in patients with chronic hepatitis C virus infection. *Antimicrob Agents Chemother.* 45(2) 517–524.

Jendželovská, Z., Jendželovský, R., Hiľovská, L., Kovaľ, J., Mikeš, J., Fedoročko, P. (2014). Single pre-treatment with hypericin, a St. John's Wort secondary metabolite, attenuates cisplatin- and mitoxantrone-induced cell death in A2780, A2780cis and HL-60 cells. *Toxicol In Vitro.* 28(7):1259-73.

Jellin, J.M., Gregory, P.J., Batz, F., Hitchen, K. (2002). *Pharmacist's Letter/Prescriber's Letter Natural Medicines Comprehensive Database.* Stockton, CA: Therapeutic Research Faculty.

Johnston, R.B., Keele, B.B., Misra, H.P., Lehmeyer, J.E., Webb, L.S., Baehner, R.L., RaJagopalan, K.V. (1975). The role of superoxide anion generation in phagocytic bactericidal activity. Studies with normal and chronic granulomatous disease leukocytes. *J Clin Invest*. 55(6):1357-72.

Josephy, P.D. (2010). Genetic variations in human glutathione transferase enzymes: significance for pharmacology and toxicology. *Hu Genomics Proteomics*. 2010:876940.

Kamerbeek, N.M., van Zwieten, R., de Boer, M., Morren, G., Vuil, H., Bannink, N., Lincke, C., Dolman, K.M., Becker, K., Schirmer, R.H., Gromer, S., Roos, D. (2007). Molecular basis of glutathione reductase deficiency in human blood cells. *Blood.* 109:3560-3566.

Karplus, P.A., Schulz, G.E. (1987). Refined structure of glutathione reductase at 1.54 A resolution. *J Mol Biol.* 195(3):701-29.

Kascakova, S., Nadova Z., Mateasik, A., Mikes, J., Huntosova, V., Refregiers, M. (2008). High level of low-density lipoprotein receptors enhance hypericin uptake by U-87 MG cells in the presence of LDL. *Photochem Photobiol*. 84:120–127.

Kenneth, M., Klemow, Andrew Bartlow., Justin, Crawford, NeiL, Kocher, Jay., Shah., and Michael, Ritsick. (2011*). Medical Attributes of St. John's Wort (Hypericum perforatum). Herbal Medicine: Biomolecular and Clinical Aspects.* Boca Raton, Florida: CRC Press Taylor & Francis.

Khalid, R. (2007). Studies on free radicals, antioxidants, and co-factors. *Clin Interv Aging*. 2(2):219–236.

Khansari, N., Shakiba, Y., Mahmoudi, M. (2009). Chronic inflammation and oxidative stress as a major cause of age-related diseases and cancer. *Recent Pat Inflamm Allergy Drug Discov*. 3(1):73-80.

Kisucka, J., Chauhan, A.K., Patten, I.S., Yesilaltay, A., Neumann, C., Van Etten, R.A., Krieger, M., Wagner, D.D. (2008). Peroxiredoxin 1 prevents excessive endothelial activation and early atherosclerosis. *Circ Res*. 103(6):598-605.

Kitiyakara, C., Wilcox, C.S. (1998). Antioxidants for hypertension. *Curr Opin Nephrol Hypertens.* 7(5):531–538.

Korsmeyer, S.J., Yin, X.M., Oltvai, Z.N., Veis-Novack, D.J., Linette, G.P. (1995) Reactive oxygen species and the regulation of cell death by the Bcl-2 gene family. *Biochim Biophys Acta*. 1271(1):63-6.

Kowluru, R.A. (2003). Effect of reinstitution of good glycemic control on retinal oxidative stress and nitrative stress in diabetic rats. *Diabetes*. 52(3):818-23.

Kraus, G.A., Pratt D, Tossberg, J., Carpenter, S. (1990). Antiretroviral activity of synthetic hypericin and related analogies. *Biochem Biophys Res Commun.* 172:149–153.

Kulaksiz-Erkmen, G., Dalmizrak, O., Dincsoy-Tuna, G., Dogan, A., Ogus, H., Ozer, N. (2013). Amitriptyline may have a supportive role in cancer treatment by inhibiting glutathione S-transferase pi (GST-π) and alpha (GST-α). *J Enzyme Inhib Med Chem*. 28(1):131-6.

Laemmli, U.K. (1970). Cleavage of structural proteins during the assembly of the head of bacteriophage T4. *Nature*. 227(5259):680–685.

Landqvist, N. (1955). On the reaction between urea and formaldehyde in neutral and alkaline Solutions III experimental studies of the rates of hydrolysis of monomethylol urea. *Acta Chemica Scandinavica.* 9(9):1466-1470.

Lavie, G., Valentine, F., Levin, B., Mazur, Y., Gallo, G., Lavie, D., Weiner, D., Meruelo, D. (1989). Studies of the mechanisms of action of the antiretroviral agents hypericin and pseudohypericin. *Proc Natl Acad Sci USA*. 6:5963–5967.

Lenard, J., Rabson, A., Vanderoef, R. (1993). Photodynamic inactivation of infectivity of human immunodeficiency virus and other enveloped viruses using hypericin and rose bengal. *Proc Natl Acad Sci USA.* 90:158–162.

Li, S., Zhang, J., Li, J., Chen, D., Matteucci, M., Curd, J., Duan, J.X. (2010). Inhibition of both thioredoxin reductase and glutathione reductase may contribute to the anticancer mechanism of TH-302. *Biol Trace Elem Res.* 136(3):294-301.

Liu, C.D., Kwan, D., Saxton, R.E., McFadden, D.W. (2000). Hypericin and photodynamic therapy decreases human pancreatic cancer in vitro and in vivo. *J Surg Res*. 93:137-143.

Lobo, V., Patil, A., Phatak, A., Chandra, N. (2010). Free radicals, antioxidants and functional foods: Impact on human health. *Pharmacogn Rev*. 4(8):118–126.

Loren, W. (1999). *A Review of the Hypothetical Biogenesis and Regulation of Hypericin synthesis via the Polyketide Pathway in Hypericum perforatum and Experimental Methods Proposed to Evaluate the Hypothesis*. Portland, OR: Portland State University.

Lu, S.C. (2013). Glutathione synthesis. *Biochim Biophys Acta*. 1830(5): 3143–3153.

Lubos, E., Loscalzo, J., Handy, D.E. (2011). Glutathione peroxidase-1 in health and disease: From molecular mechanisms to therapeutic opportunities. *Antioxid Redox Signal*. 15(7):1957–1997.

Luksiene, Z. (2003). Photodynamic therapy: mechanism of action and ways to improve the efficiency of treatment. *Medicina (Kaunas).* 39(12):1137-50.

Maduray, K., and Davids, L.M. (2011) The anticancer activity of hypericin in photodynamic therapy. *J Bioanal Biomed.* 6:1-4.

Mandal A. (2016). Antioxidant Enzyme Systems. http://www.news-medical.net/ health / Antioxidant-Enzyme-Systems.aspx, 9/11/2016.

Mannervik, B., Danielson, U.H. (1988). Glutathione transferases-structure and catalytic activity. *CRC Crit Rev Biochem*. 23(3):283-337.

Martínez, M.C., Andriantsitohaina, R. (2009). Reactive nitrogen species: molecular mechanisms and potential significance in health and disease. *Antioxid Redox Signa*. 11(3):669-702.

Massaad, C.A., Klann, E., (2011). Reactive oxygen species in the regulation of synaptic plasticity and memory. *Antioxid Redox Signal*. 14(10): 2013–2054.

Massey, V., Williams C.H, Jr. (1965). On the reaction mechanism of yeast glutathione reductase. *J Biol Chem*. 240(11):4470–448.

Mavis, R.D., Stellwagen, E. (1968). Purification and subunit structure of glutathione reductase from bakers' yeast. *J Biol Chem*. 243(4):809-14.

Mecocci, P., MacGarvey, U., Kaufman, A.E., Koontz, D., Shoffner, J.M., Wallace, D.C., Beal, M.F. (1993). Oxidative damage to mitochondrial DNA shows marked age-dependent increases in human brain. *Ann Neurol*. 34(4):609-16.

Meruelo, D., Lavie, G., Lavie, D. (1988). Therapeutic agents with dramatic antiretroviral activity and little toxicity at effective doses: aromatic polycyclic diones hypericin and pseudohypericin. *Proc Natl Acad Sci USA*. 85(14):5230-4.

Mikeš, J., Hýžd'alová, M., Kočí, L., Jendželovský, R., Koval', J., Vaculová, A. (2011). Lower sensitivity of FHC fetal colon epithelial cells to photodynamic therapy compared to HT-29 colon adenocarcinoma cells despite higher intracellular accumulation of hypericin. *Photochem Photobiol Sci*. 10:626–632.

Mikeš, J., Kleban, J., Sacková V., Horváth, V., Jamborová, E., Vaculová, A. (2007). Necrosis predominates in the cell death of human colon adenocarcinoma HT-29 cells treated under variable conditions of photodynamic therapy with hypericin. *Photochem Photobiol Sci*. 6:758–766.

Mills, G.C. (1957). Hemoglobin catabolism. I. Glutathione peroxidase, an erythrocyte enzyme which protects hemoglobin from oxidative breakdown. *J Biol Chem*. 229(1):189-97.

Moraleda, G., Wu, T.T., Jilbert, A.R., Aldrich, C.E., Condreay, L.D., Larsen, S.H., Tang, J.C., Colacino, M., Mason, W.S., (1993). Inhibition of duck hepatitis B virus replication by hypericin. *Antivir Res.* 20:235–247.

Muller, E.G. (1996). A glutathione reductase mutant of yeast accumulates high levels of oxidized glutathione and requires thioredoxin for growth. *Mol Biol Cell.* 7(11):1805–1813.

Murad, F. (1996). Signal transduction using nitric oxide and cyclic guanosine monophosphate. *JAMA.* 279:1189–1189.

Mustacich, D. and Powis, G. (2000). Thioredoxin reductase. *Biochem J*. 346(Pt 1):1–8.

Nishiuchi, T., Utsumi, T., Kanno, T., Takehara, Y., Kobuchi, H., Yoshioka, T., Horton, A. A., Yasuda, T., Utsumi, K. (1995). Inhibition of neutrophil superoxide generation by hypericin, an antiretroviral agent. *Arch Biochem Biophys.* 323(2):335-42.

Ogüs, H., Ozer N. (1998). Purification of NADPH-free glutathione disulfide reductase from human erythrocytes. *Protein Expr Purif*. 13(1):41-4.

Ott, M., Gogvadze, V., Orrenius, S., Zhivotovsky, B. (2007). Mitochondria, oxidative stress and cell death. *Apoptosis.* 12(5):913-22.

Outten, C.E., Culotta, V.C. (2013). Alternative Start Sites in the *S. cerevisiae* GLR1 Gene are Responsible for Mitochondrial and Cytosolic Isoforms of Glutathione Reductase. *J Biol Chem*. 27:279(9).

Pacher, P., Beckman, J.S., Liaudet L. (2007). Nitric oxide and peroxynitrite in health and disease. *Physiol Rev.* 87(1):315-424.

Pastrana-Mena, R., Dinglasan, R.R., Franke-Fayard, B., Vega-Rodríguez, J., Fuentes-Caraballo, M., Baerga-Ortiz, A., Coppens, I., Jacobs-Lorena, M., Janse C.J., Serrano, A.E. (2010). Glutathione reductase-null malaria parasites have normal blood stage growth but arrest during development in the Mosquito. *J Biol Chem*. 285(35):27045-56.

Pence, S., Erkutlu, I., Kurtul, N., Bosnak, M., Alptekin, M., Tan, U. (2009). Antiepileptogenic effects of glutathione against increased brain ADA in PTZ-induced epilepsy. *Int J Neurosci*. 119(5):616-29.

Percy, M.E. (1984).Catalase: an old enzyme with a new role. *Can J Biochem Cell Biol*. 62(10):1006-14.

Perry, J.J., Fan, L., Tainer, J.A. (2007). Developing master keys to brain pathology, cancer and aging from the structural biology of proteins controlling reactive oxygen species and DNA repair. *Neuroscience*. 145(4):1280-99.

Petrich J.W. (2000) Excited-state intramolecular H-atom transfer in nearly symmetrical perylene quinones: Hypericin, hypocrellin, and their analogues. *Int Rev Phys Chem.* 19:479–500.

Pocernicha, C.B. and Butterfield D.A. (2012). Elevation of glutathione as a therapeutic strategy in Alzheimer disease. *Biochim Biophys Acta*. 1822(5):625–630.

Powers, S.K. and Jackson, M.J. (2008). Exercise-induced oxidative stress: cellular mechanisms and impact on muscle force production. *Physiol Rev*. 88(4):1243-1276.

Raedschelders, K., Ansley, D.M., Chen, D.D.Y. (2012). The cellular and molecular origin of reactive oxygen species generation during myocardial ischemia and reperfusion. *Pharmacol Ther*. 133:230–25.

Ren, B., Huang, W., Akesson, B., Ladenstein, R. (1997). The crystal structure of seleno-glutathione peroxidase from human plasma at 2.9 A resolution. *J Mol Biol*. 268(5):869-85.

Roum, J.H., Buhl, R., McElvaney, N.G., Borok, Z., Crystal, R.G. (1985). Systemic deficiency of glutathione in cystic fibrosis. *J Appl Physiol.* 75(6):2419-24.

Rubio, N., Coupienne, I., Di, V.E., Heirman I., Grooten J., Piette J. (2012). Spatiotemporal autophagic degradation of oxidatively damaged organelles after photodynamic stress is amplified by mitochondrial reactive oxygen species. *Autophagy*. 8:1312–132.

Sattler, S., Schaefer, U., Schneider, W., Hoelzl, J., Lehr, C.M. (1997). Binding, uptake, and transport of hypericin by Caco-2 cell monolayers. *J Pharm Sci*. 86: 1120–1126.

Schrader, M., Fahimi, D. (2006). Peroxisomes and oxidative stress. *Biochim Biophys Acta*. 1763(12):1755-66.

Scibior, D., Czeczot, H. (2006).Catalase: structure, properties. *Functions Postepy Hig Med Dosw (Online).* 60:170-80.

Seefeldt, T., Dwivedi, C., Peitz, G., Herman, J., Carlson, L., Zhang, Z., Guan, X.J. (2005). Acetylamino-3-[4-(2-acetylamino-2-carboxyethyl-) phenylcarbamoyl sulfanyl] propionic acid and its derivatives as a novel class of glutathione reductase inhibitors. *Med Chem*. 48(16):5224–5231.

Segel, I.R. (1975*). Enzyme Kinetics: Behavior and Analysis of Rapid Equilibrium and Steady-State Enzyme Systems*. Toronto: Wiley.

Sheehan, D., Meade, G., Foley, V.M., Dowd, C.A. (2001). Structure, function and evolution of glutathione transferases: implications for classification of non-mammalian members of an ancient enzyme superfamily. *Biochem J*. 360:1–16.

Siboni, G., Weitman, H., Freeman, D., Mazur, Y., Malik, Z., Ehrenberg, B. (2002). The correlation between hydrophilicity of hypericins and helianthrone: internalization mechanisms, subcellular distribution and photodynamic action in colon carcinoma cells. *Photochem Photobiol Sci*. 1(7):483-91.

Sienko, S., Eis-Hübinger, A.M., Schneweis, K.E. (1991). The role of free radical scavengers, inhibitors of prostaglandin synthesis, and hypomethylating agents in reactivation of latent herpes simplex virus. *Med Microbiol Immunol*. 180(5):249-59.

Smeyne, M., Smeyne, R.J. (2013). Glutathione metabolism and Parkinson's disease. *Free Radic Biol Med*. 62:13-25.

Sørensen, M.G., Karsdal, M.A., Dziegiel, M.H., Boutin, J.A., Nosjean, O., Henriksen, K. (2010). Screening of protein kinase inhibitors identifies PKC inhibitors as inhibitors of osteoclastic acid secretion and bone resorption. *BMC Musculoskelet Disord*. 11(250):1-11.

Staffeldt, B., Kerb, R., Brockmöller, J., Ploch, M., Roots, I. (1994). Pharmacokinetics of hypericin and pseudohypericin after oral intake of the hypericum perforatum extract LI 160 in healthy volunteers. *J Geriatr Psychiatry Neurol*. 10(3):114-8.

Suzuki, O., Oya, M., Bladt, S., Wagner, H. (1984). Inhibition of monoamine oxidase by hypericin. *Planta Med*. 2:272.

Takenaka, A., Kizawa, K., Hata, T., Sato, S., Misaka, E., Tamura, C., Sasada, Y. (1988). X-ray study of baker's yeast lipoamide dehydrogenase at 4.5 A resolution by molecular replacement method. *J Biochem*. 103(3):463-9.

Tandoğan, B., Ulusu, N. (2007). The inhibition kinetics of yeast glutathione reductase by some metal ions. *J Enzyme Inhib Med Chem.* 22(4):489-95.

Tang, J., Colacino, J.M., Spitzer, W. (1990). Virucidal activity of hypericin against enveloped and non-enveloped DNA and RNA viruses. *Antivir Res.* 3:313–326.

Tatsuzawa, H., Maruyama, T., Hori, K. (1999). Singlet oxygen as the principal oxidant in myeloperoxidase-mediated bacterial killing in neutrophil phagosomes. *Biochim Biophys Res Commun*. 262:647–50.

Tauber, A.I., Borregaard, N., Simons, E., Wright, J. (1983). Chronic granulomatous disease: a syndrome of phagocyte oxidase deficiencies. *Medicine (Baltimore).* 62(5):286-309.

Thomas, C., MacGill, R.S., Miller, G.C., Pardini, R.S. (1992). Photoactivation of hypericin generates singlet oxygen in mitochondria and inhibits succinoxidase. *Photochem Photobiol*. 55(1):47-53.

Townsend, D.M. and Tew, K.D. (2003). The role of glutathione-S-transferase in anti-cancer drug resistance. *Oncogene.* 22:7369-737.

Tuna, G., Kulaksiz Erkmen, G., Dalmizrak, O., Dogan, A., Ogus, H., Ozer, N. (2010). Inhibition characteristics of hypericin on rat small intestine glutathione-S-transferases. *Chem Biol Interact*. 188(1):59-65.

Turk, S., Kulaksiz Erkmen, G., Dalmizrak, O., Ogus, H., Ozer, N. (2015). Purification of glutathione S-transferase pi from erythrocytes and evaluation of the inhibitory effect of hypericin. *Protein J*. 34(6):434-43.

Untucht-Grau, R., Schirmer, R.H., Schirmer, I., Krauth-Siegel, R.L. (1981). Glutathione reductase from human erythrocytes: amino-acid sequence of the structurally known FAD-binding domain. *Eur J Biochem*. 120(2):407-19.

Valko, M., Rhodes, C.J., Moncol, J., Izakovic, M., Mazur, M. (2006). Free radicals, metals and antioxidants in oxidative stress-induced cancer. *Chem Biol Interact*. 160(1):1-40.

Wei, Y.H., Ma, Y.S., Lee, H.C., Lee, C.F., Lu, C.Y. (2001). Mitochondrial theory of aging matures--roles of mtDNA mutation and oxidative stress in human aging. *Zhonghua Yi Xue Za Zhi (Taipei).* 64(5):259-70.

Wendell, P.L. (1968). Distribution of glutathione reductase and detection of glutathione-cysteine transhydrogenase in rat tissues. *Biochim Biophys Acta.* 159(1):179-81.

Weydert, C.J., Cullen, J.J. (2010). Measurement of superoxide dismutase, catalase and glutathione peroxidase in cultured cells and tissue. *Nature Protocols*. 5(1):51-66.

Willmore, W.G., Storey, K.B. (2007). Purification and properties of glutathione reductase from liver of the anoxia-tolerant turtle Trachemys Scripta Elegans. *Biochem*. 297: 139.

Wilson, C.M. (1979). Studies and critique of Amido Black 10B, Coomassie Brilliant Blue R and fast Green FCF as stains for proteins after polyacrylamide gel electrophoresis. *Anal Biochem*. 96(2):263-273.

Wruck, C.J., Fragoulis, Gurzynski, Brandenburg, L.O., Kan, Y.W., Chan, K., Hassenpflug, J., Freitag-Wolf, S., Varoga, D., Lippross, S., Pufe, T. (2011). Role of oxidative stress in rheumatoid arthritis: insights from the Nrf2-knockout mice. *Ann Rheum Dis*. 70(5):844-50.

Yee, K.K., Soo, K.C., Olivo, M. (2005). Anti-angiogenic effects of Hypericin-photodynamic therapy in combination with Celebrex in the treatment of human nasopharyngeal carcinoma. *Int J Mol Med*. 16:993-1002.

Young, I.S., Woodside, J.V. (2001). Antioxidants in health and disease. *J Clin Pathol.* 54(3):176-86.

Yu, E., Mercer, J., Bennett, M. (2012). Mitochondria in vascular disease. *Cardiovascular Research*. 95:173–182.

Yu, J., Zhou, C.Z. (2007). Crystal structure of glutathione reductase Glr1 from the yeast *Saccharomyces cerevisiae. Proteins.* 68(4):972-9.

Yuan, L., Kaplowitz, N. (2009). Glutathione in liver diseases and hepatotoxicity. *Mol Aspects Med*. 30(1-2):29-41.

Zhang, Q., Li, ZH., Li, Y.Y., Shi, S.J., Zhou, S.W., Fu, Y.Y., Zhang, Q., Yang, X., Fu, R.Q., Lu, L.C. (2015). Hypericin-photodynamic therapy induces human umbilical vein endothelial cell apoptosis. *Sci Rep*. 5:18398.

Zhao, Y., Seefeldt, T., Chen, W., Wang, X., Matthees, D., Hu, Y., Guan, X. (2009). Effects of glutathione reductase inhibition on cellular thiol redox state and related systems. *Arch Biochem Biophy*. 485(1):56–62.